Comparisons of the Structural Response of a Test Article Excited by DFAT™ Diffuse and Non-Diffuse Acoustic Fields

by
Marcos A. Underwood, PhD
Tu'tuli Enterprises and
MSI DFAT Chief Scientist

Abstract

This paper discusses the results from Direct Field Acoustic Tests (DFAT™) performed at MSI DFAT to evaluate how effectively nearly diffuse (low coherence) and non-diffuse (high coherence) acoustic fields, using MIMO and MISO control, excite the structural resonances of a test article. The criteria used is to compare the frequency of resonances excited by the resulting acoustic fields to what Modal Analysis predicts the modes of vibration, their natural frequencies, and damping to be. Test results from using the various acoustic fields created by DFAT™ to excite the test article (test panel), in the form of PSDs obtained from accelerometers mounted on the test panel are analyzed. This analysis is used to determine the relative ability of the various acoustic fields to properly excite test articles by examining how well the resonances shown by the PSDs match the damped resonant frequencies predicted by Modal Analysis.

I. Introduction

The primary goal of testing was to use DFAT™ [15] to determine how effectively nearly diffuse (low coherence), non-diffuse (high coherence), non-diffuse directed coherent acoustic field (directed coherent field) specified by phase and high-coherence settings in their reference SDM [4,11], and MISO generated acoustic fields excite the structural resonances of an aluminum honeycombed 4'x8' test panel (panel) [4]. The paper presents an analysis of the results from 4 tests performed to investigate the dependence of the panel's acceleration PSD response as a function of the reference SDM coherence and phase settings [9] used for the creation of the various acoustic fields [14] used to excite the panel. The study found that when using the same acoustic OA SPL and reference spectrum Profile: 1) the Reference SDM Coherence and Phase Settings for the 3 MIMO tests have a fundamental effect on the nature of the panel's response; 2) the 3 non-diffuse tests consistently miss properly exciting significant resonances and that their panel responses exhibit enhancement/cancellation and "phantom resonance" response effects [14]; and 3) that MISO control acoustic fields performed the poorest [4], due to its lack of coherence and phase control [14].

As a result of testing with diffuse and non-diffuse fields, using both MIMO and MISO control, the power needed to accomplish the 4 tests was studied by analyzing the drive(s) signal levels used to create the various acoustic fields that were used to excite the test panel. The power study found that MIMO diffuse acoustic field testing only requires 1.3 dB of additional power over using MISO control, thus providing a good cost/performance tradeoff by providing the benefits of uniform diffuse acoustic field testing, with low additional power requirements, which is due to the modern optimal adaptive MIMO control and optimized loudspeaker designs used by MSI DFAT technology [14].

II. Testing Configurations

The testing to support the described activity was performed using MSI DFAT's 8x8 speaker stack configuration with 24 control microphones using SD Jaguar MIMO and MISO control [7,9,11-14] to create: 1) a nearly diffuse acoustic field [2] such that the relative coherence between control microphones was low, approximating the relative coherence obtained from RATF testing, which is high at low frequencies for microphones that are close, approximating a sinc^2 curve [2,4] that falls off at higher frequencies and as the distance between control microphones increase [12,14]; 2) a non-diffuse acoustic field such that the relative coherence between control microphones is initially high, but drops to a 0.6 nominal coherence at higher frequencies to 10 kHz; 3) an acoustic field containing a directed coherent acoustic field component at lower frequencies normal to the test panel's surface, with a 30% diffuse content, as another example of nearly coherent excitation, where the initial coherence is also

high at the lower frequencies where the directional field dominates, but which drops to 0.7 at higher frequencies; and 4) an acoustic field obtained from a MISO controlled acoustic test [12-14] that uses a single drive for all speakers, where the average of the 24 control-microphone PSD's is controlled to the same acoustic spectrum, as for the first 3 tests, as yet as another example of a non-diffuse acoustic field. The reference spectrum used for all 4 tests, which is at 138.5 OA SPL, and whose spectra are shown in the following Fig. 1a, in equivalent narrowband PSD and 1/3rd Octave SPL Spectra forms [12,13].

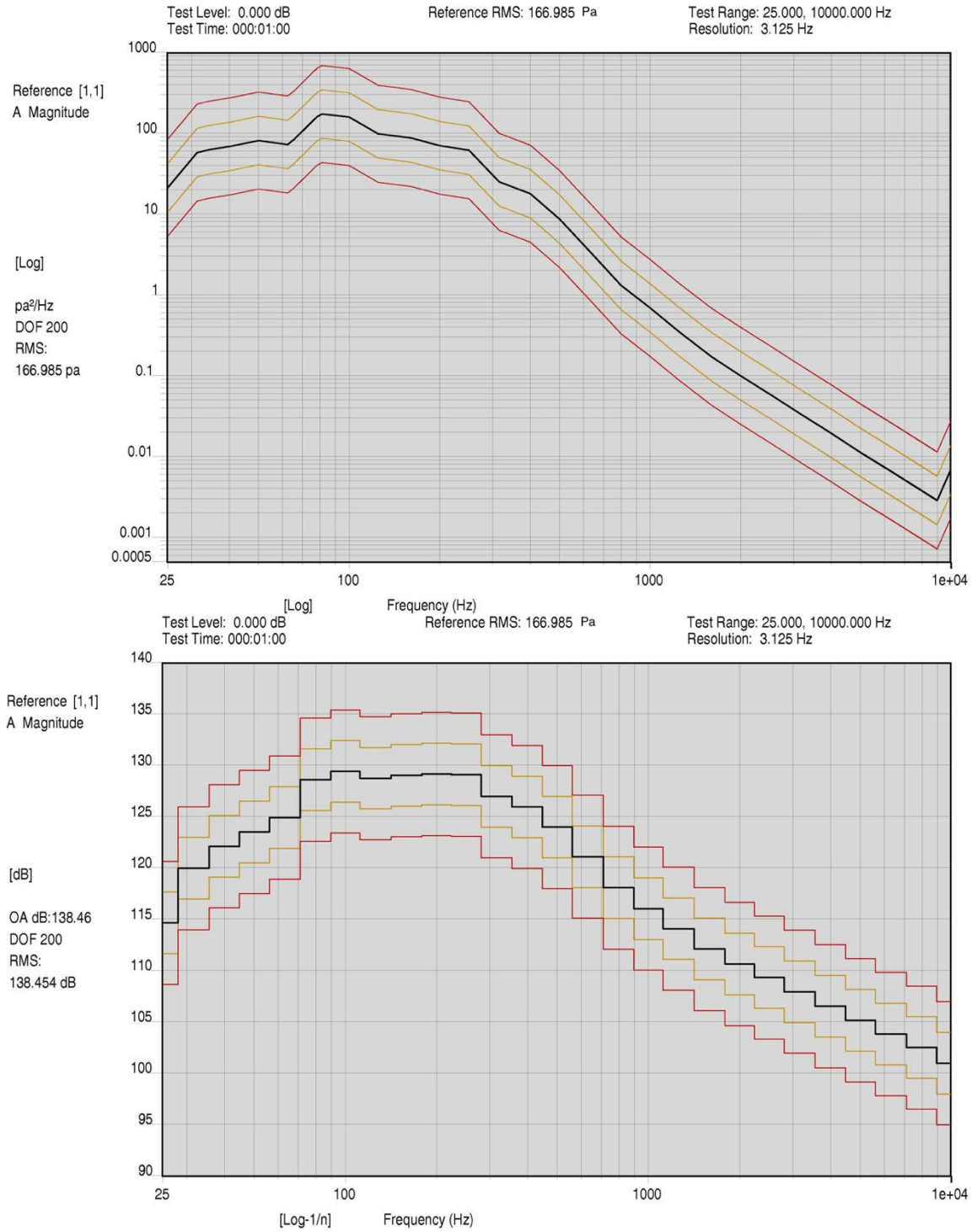

Fig. 1a: Reference Spectra Used for all 24 Control Channels with Discussed Acoustic Tests

The 8x8 stack configuration with 8-drives and 24 control microphones were used for the described testing. The 8x8 configuration consists of 8 MP-150 mid/high transducers stacked 6’ tall and 8 MP-21 subwoofers driven by 8 independent drives. An elliptic shaped microphone configuration was used that surrounds the panel test article, which was suspended from the ceiling, with a damping point mass at its top, and anchored to the floor with bungee cords near the center of the 8x8 configuration and microphones, as shown in Fig. 2. The following Fig. 1b shows the 8x8 speaker configuration, elliptic control microphone configuration and their numbers, and where the test panel was located, shown as an 8’ horizontal arrow at their center. The test panel and how it was instrumented will be discussed more fully later in this section.

The microphones were spaced 18” apart, with their heights randomized within +/- 1’ to avoid symmetries and avoid being arranged along nodes of the acoustical modes that may be present during acoustic testing [12]. These changes in height result in an average spacing between microphone of 2’, but with their lateral spacing still at 1.5’. The microphone ellipse shown in Fig. 1b was 14’ by 12’ and nearly circular. The distance between microphones that controls their relative coherence is their secant distance within the microphone ellipse, as discussed later.

Other testing configurations were also run that used a rotated panel configuration in which the panel suspended at the center of speaker circle was rotated 30^{o} counter-clockwise from what is shown in Fig. 1b, as well as 4-drive versions of all of the described tests. No significant differences in the response behavior from what is discussed in this paper were found, and thus it was decided to focus on the test results from the four configurations that have been described. What was established instead, was that the SDM settings of the coherence and phase used to specify the acoustic fields that was used for testing had the most significant effect. However, the utilized power results from all 12 tests that were run was used to obtain a more complete understanding of what the power utilization is as a function of testing configuration. Those results are presented in the last section of this paper.

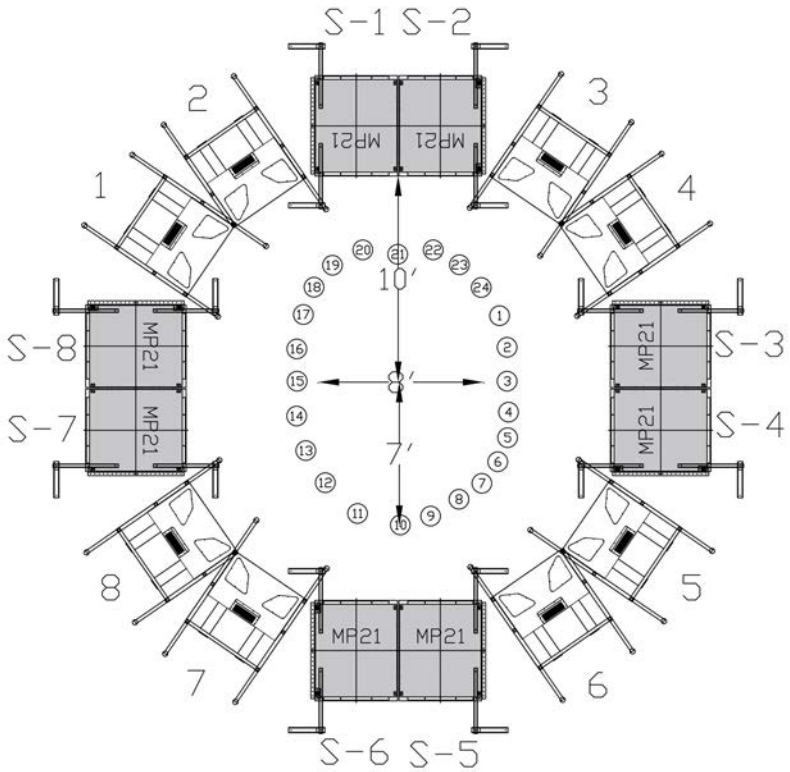

Fig. 1b: 8x8 Stack, Test Article, & Elliptic Control Microphone Configuration

The underlying basic idea of the four tests that are discussed is to characterize the structural response characteristics by PSDs obtained from accelerometers mounted on the panel at chosen locations as a result of being excited by the discussed 4 acoustic-fields. A baseline of the desired response characteristics of the panel was obtained by

performing a Modal Test and Analysis to determine the first 25 modes, up to 400 Hz, of which only the first 16 modes from 40 Hz to 250 Hz were used to correlate with what was found during testing, since lower frequency modes are the most significant from a structural stress/strain viewpoint. Modal Testing and Analysis, was performed after acoustic testing had concluded, that identified the damped resonances of the panel as a baseline of what should be excited and identified during the acoustic testing, using each of the discussed four types of acoustic fields.

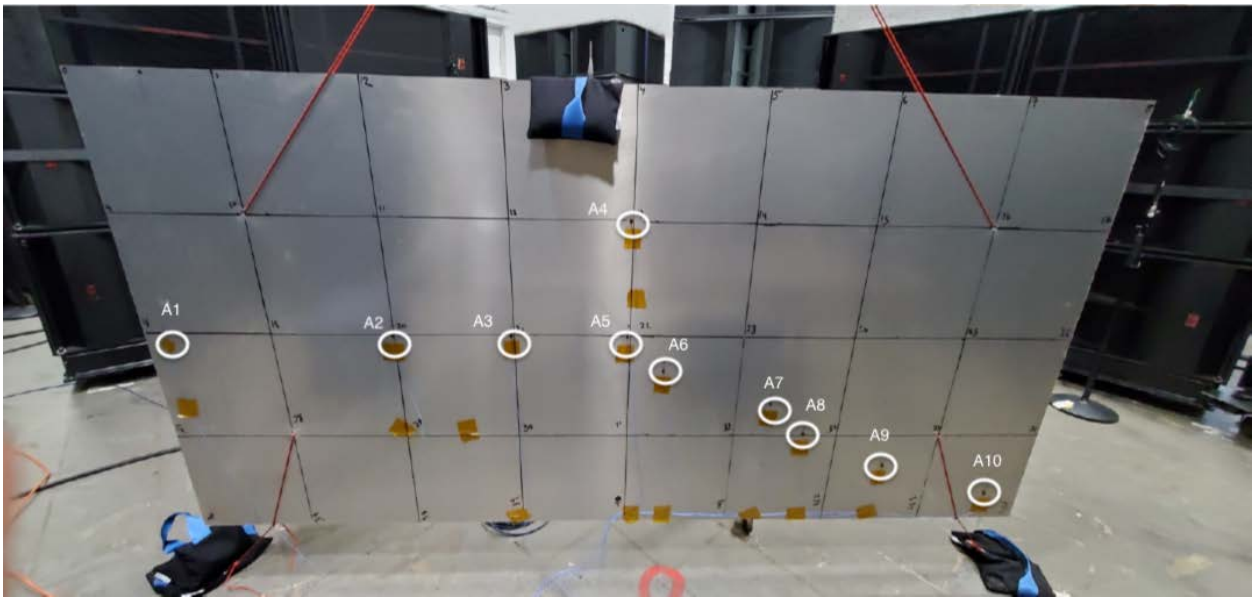

Fig. 2: Aluminum Honeycombed 4'x8' Panel Plate Showing Accelerometer Placement

Accelerometer Locations

Fig. 3: Accelerometer Placement on Panel

	4	8	12	16	20	24	28	32	36	40	44	48	52	56	60	64	68	72	76	80	84	88	92	96
0																								
4																								
8																								
12												**4**												
16																								
20																								
24	**1**					**2**			**3**			**5**												
28													**6**											
32																**7**								
36																		**8**		**9**				
40																								
44																								**10**
48																								

Fig. 4: Coordinates of Accelerometer locations on Panel

	X	Z
1	2	24
2	24	24
3	36	24
4	48	12
5	48	24
6	52	28
7	64	32
8	72	36
9	82	36
10	**94**	**44**

A photograph of the test panel is shown in Fig. 2. The placement of the 10-response accelerometer that were mounted on the panel, for both the acoustic and modal testing, are indicated by white circles and labels shown in Fig. 2 and numbers in Fig. 3. Figs. 3 and 4 further show the 10 accelerometer's coordinates in inches, for both the acoustic tests and the Modal Testing and Analysis discussed in later sections.

The vertices of the 1' squares shown drawn on the panel shown by Fig. 2 constituted 45 points excited by blows by a hammer instrumented with a force transducer, to perform the Modal Test, from which data the Modal Analysis was performed. These 45 hammer excitation points were labeled 0 through 44, as shown in Fig. 2.

III. Description of the Discussed Testing Methodology

1. The four tests discussed, which used the same reference shown in Fig. 1a, were as follows:
   a. Test R5A was configured to use 8 independent drives for the 8x8 configuration. 8x24 Rectangular MIMO control was used [4,8,11-14]. The initial reference SDM coherence and phase [7,9,10], between the 24 control-microphones, was set to 0.0 to approximate a diffuse acoustic field [12-14]. A subsequent characterization low-level test determined the Optimized Reference SDM [14] and Impedance Matrix [7,11] to use for the actual test. Due to MIMO control, the response PSD's and 1/3rd octave SPL spectra of the 24 control microphones was nearly uniform in matching each other and their reference in Fig. 1a. The relative coherence between control microphones approximates what is expected from a diffuse acoustic field [2,4,14], both of which demonstrated by the results to be shown.
   b. Test R5B was configured to use 8 independent-drives as was described for test R5A. The initial reference SDM coherence and phase between the 24 control microphones was initially set to 0.6 and 0.0^{o} to attempt to approximate a non-diffuse acoustic field. The subsequent characterization low-level test determined the Optimized Reference SDM and Impedance Matrix to use for the actual test, whose results showed lesser control microphone PSD uniformity than test R5A and with the expected larger coherence between control microphones to 10 kHz, as will be shown.
   c. Test R4A was configured to use 8 independent drives as was described for the previous two tests. Since the purpose of test R4A was to create a directed highly coherent and in-phase acoustic field at the lower frequencies, with some diffuse content for all frequencies, the initial reference SDM had a more complex setup for its off-diagonal phase and coherence terms [9]. The initial reference SDM coherence between the 24 control microphones was set to 0.7, but with its corresponding relative phase terms set to create a directed acoustic field moving approximately towards the panel, normal to its surface, from its front and moving away from the panel from its rear in the positive portion of its oscillation. The subsequent characterization low-level test determined the Optimized Reference SDM and Impedance Matrix to use for the actual test that followed, whose test results also showed a lesser control PSD uniformity than test R5A, but slightly better than R5B, and with the expected larger coherence between control microphones than shown by previous tests for all frequencies to 10 kHz.
   d. Test R5E was configured to use 1 drive in a MISO configuration [4,14] with the same 24 control microphones, as in tests R5A, R5B, and R4A, and the single drive, using average control, was routed to all speakers in the 8x8 speaker stack configuration. The resulting acoustic field was also non-diffuse [4,14], with the associated natural acoustic modal responses present, due to the lack of MIMO control, with much larger variation of the spectral responses, PSD and 3rd octave band SPL spectrum associated with the 24 control microphones, than the other three tests [4,12-14].

IV. Results from Tests R5A, R5B, R5E, and R4A

1. For test R5A the following results were obtained:

As can be seen, Fig. 5 shows excellent agreement of the average of all 24 control microphones and their reference in both 1/3rd Octave SPL and PSDs forms. Fig. 6 also shows excellent control microphone PSD uniformity for all 24 control microphones, typical of what has been seen previously [13,14] with the 8x8 speaker stack configuration diffuse testing. Fig. 7a shows an approximate sinc^2 function shape coherence [2,4,14] for nearby microphone pairs, like between 1 and 2 and 1 and 24, for low frequencies, and near zero coherence between control microphones 1 and 2, through 1 and 24, for the higher frequencies for all microphone pairs, but with large variance in coherence values, as is characteristic of a low value coherence less than or equal to 0.4 [1].

a. Average Control in 1/3rd Octave and Narrowband PSD Spectra Formats

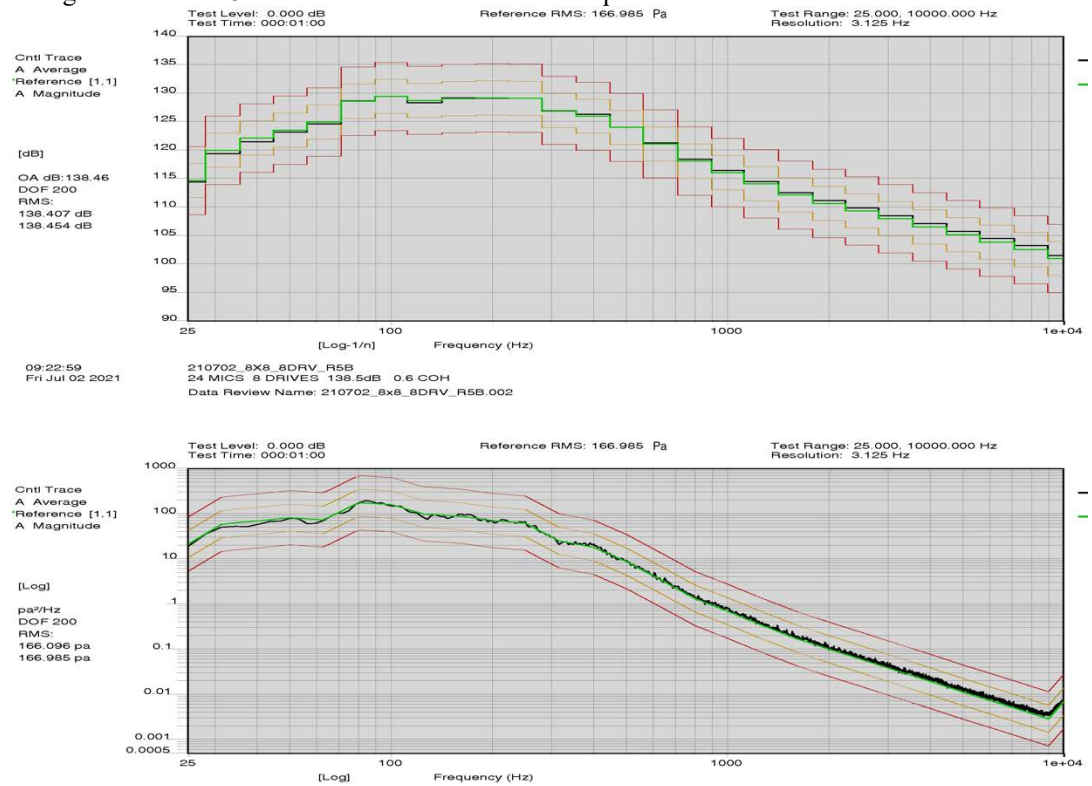

Fig. 5: Control Average as 1/3rd Octave SPL and PSD

b. Control PSDs, Coherence, and Phase

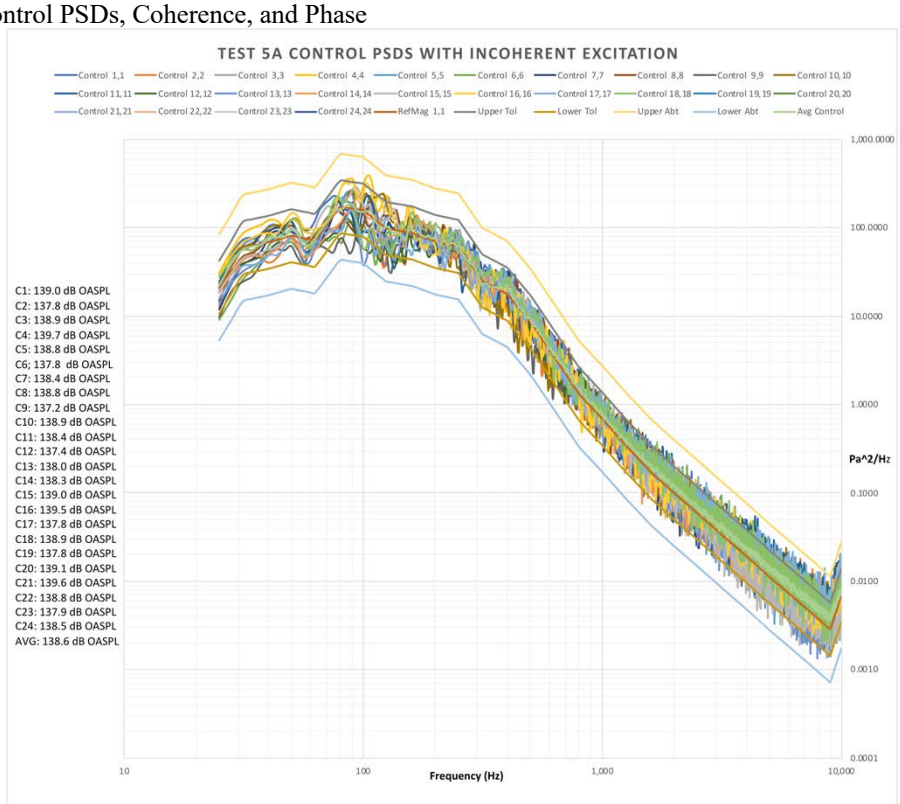

Fig. 6: Test R5A PSDs from 24 Control Microphones

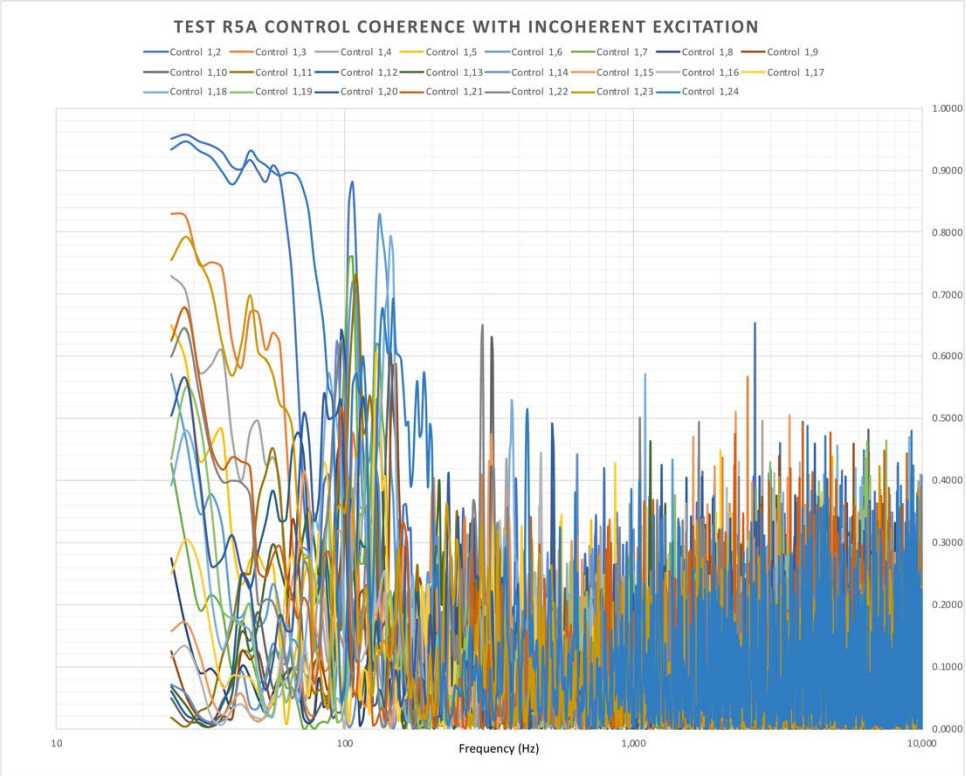

Fig. 7a: Test R5A Control Coherence for top row of SDM

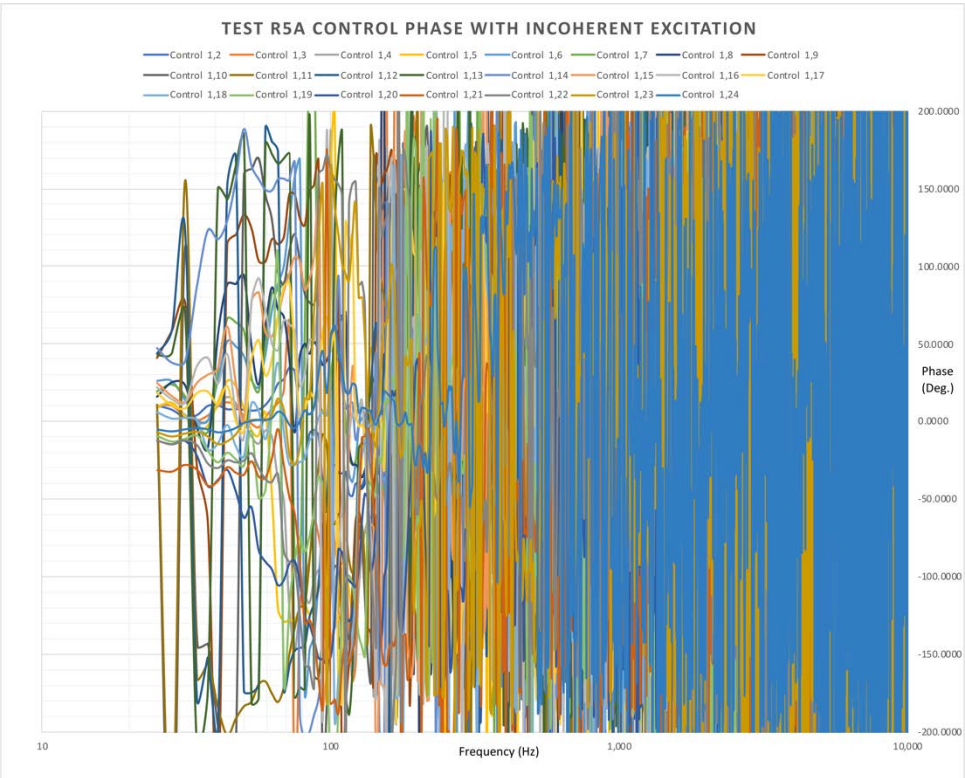

Fig. 7b: Test R5A Control Phase for top row of SDM

Fig. 7b demonstrates that the relative phase is consistent with the low coherence shown by Fig. 7a, by the random phase character that it displays [1] for all frequencies. In the following, a small "tutorial" of the meaning of the measured relative coherence and phase between microphone pairs is presented that will discuss those issues in more detail, which should help to better understand the content of Figs. 7a and 7b.

c. What Relative Coherence Measures and its Importance to DFAT™ testing

Relative coherence, as used for MIMO DFAT™, is a measure of the statistical independence between the instantaneous sound pressure levels measured by pairs of control microphones [1,4,9,10], as a function of frequency, where a value of 1 means that the measurements are completely dependent and 0 means they are completely independent at particular frequencies. The measured value of coherence at a particular frequency, f_c, is related to the square of the peak of the normalized cross-correlation function between the measured output of microphone pairs that've been passed through a narrow band pass filter, with center frequency f_c, and a narrow band-pass shape that depend on the FFT resolution and spectral window that are used [2]. The waveforms from such band-pass filters resemble sinusoids with random amplitudes, as can be easily seen with an appropriate band-pass filter and oscilloscope. Their cross-correlation functions resemble delayed (by an amount related to the relative phase between microphone outputs at f_c) decaying co-sinusoids, with a peak[2] amplitude related to the coherence at f_c [1,7].

In that manner, measured coherence between microphones pairs, which are part of an array of microphones that are located uniformly within an acoustic field, as is used to control DFAT™, is a measure of how diffuse an acoustic field is [4,14], i.e. how random the incidence phase between microphone outputs is, as is reported by numerous papers and presentations on the subject and its use to measure how diffuse an acoustic field is [2,4,14]. The larger number of control microphones that can be used to determine coherence as a function of spatial location, the more accurate that statement is [1]. Also, the variance of measured coherence and phase are inversely proportional to the magnitude of coherence, in a non-linear fashion [1], which leads to the random scatter we see in Fig. 7a for the measured coherence at the higher frequencies, where any measured coherence below 0.4 is essentially zero. In a similar manner [1,7,11], the variance of measured phase is also inversely proportional the value of coherence non-linearly as shown in Fig. 7b for all frequencies, which exhibit a random scatter of the value of phase for all frequencies, and which supports the fact that the associated coherence is nearly zero, as has been discussed. The variance of coherence and phase, as a function of coherence is discussed in [1,7,11] in greater detail.

With regards to testing a structure that is excited by a nearly diffuse (incoherent) acoustic field, it's as if the structure is being excited by a distributed force field, with a large number of uncorrelated exciters with random angles of incidence [14]. A structure tested with a non-diffuse (highly coherent) acoustic field, on the other hand, would behave as if the structure is being excited by a distributed force field, with many correlated exciters, with nearly identical fixed angles of incidence [14]. It should be clear that a diffuse acoustic field is better at exciting all of the externally excitable resonances of a given structure than a non-diffuse acoustic field, which will be demonstrated by the test article response results discussed in later sections.

d. Examination of Figs. 7a and 7b

Note that for frequencies near 25 Hz in Fig. 7a, we see the highest coherence is achieved for microphone pairs [1,2] and [1,24], where the measured coherence reduces monotonically for pairs [1,3] through pairs [1,9] and lower still for pairs [1,10] through [1,15], while increasing back to nearly the value of 0.95 for microphone pairs [1,24], which is very close to the value of microphone pair [1,2], as the microphone ellipse is traversed.

The notable fact here is that the ¼ wavelength of sound at 25 Hz (at sea level) is 11.25 ft. (3.44 m), which is close to 11.2' (3.41 m), the approximate secant distance between microphones 1 and 10, that is close to the first null of the spatial normalized cross-correlation function for 25 Hz band-pass filtered sound, as explained previously, between microphone pairs as a function of their separation distance for 25 Hz sound, which coherence at 25 Hz represents. This is reflected by the low coherence value at 25 Hz for the pairs [1,10]- [1,15] of about 0.05 that Fig. 7a shows.

Additionally, the coherence at lower frequencies, for microphone pairs separated by less than a ¼ wavelength, cannot be lowered by closed-loop MIMO control below a certain value that's due to the physics of sound pressure waves, but which is noticeably lower than what is predicted by open-loop measurements of relative coherence in RATFs [2]. The high level of coherence shown in Fig. 7a, for microphones that are close, is a result of the fact that

for microphone spacings less than a ¼ wavelength, the sound pressure levels, as measured by the microphones, are statistically dependent (not uncorrelated even in diffuse fields) to varying degrees depending on their distance, in a manner that to a first-order is approximately inversely proportional to their separation distance, as previously discussed. This fact is reflected by the coherence values shown in Fig. 7a for pairs [1,2] through [1,9] at 25 Hz, in that as the secant distance between respective pairs of control microphones increase by about 1.25'for each pair, their respective coherence declines. This result does not yet appear reported in the literature [2].

Fig. 7a also shows that the measured coherence between microphone pairs shown by Test R5A is only approximately described by a $sinc^2$, $(sin(kr)/kr)^2$ [2], as functions of frequency and separation, like what is typically measured in open-loop reverberation chambers (under very carefully controlled conditions [2]) for microphone pairs that are close (on the order of 18" or less) and distant from sound sources [2]. This occurs, because again, MIMO DFAT™ provides closed-loop control of coherence (and phase) [14] that's not available for RATF testing, and that there are multiple sound sources close to the control microphones. MIMO acoustic, which provides closed-loop control of multiple loudspeaker outputs, reduces the coherence between control microphones, as a function of frequency, to values lower than predicted by the classical $sinc^2$ function analysis used for RATF acoustic testing [2].

This is a result of the Jaguar's unique MIMO Acoustic optimal adaptive closed-loop control, which with multiple drives and speaker stacks, provides a more compressed function than the $sinc^2$ function, as seen in Fig. 7a, for the coherence between microphones as a function of frequency, that achieves very low values of coherence at 25 Hz. The fact that the coherence between microphones drops below 0.05 for pairs [1,10] through [1,15] at 25 Hz is reflected in the large variance of phase we see at frequencies as low as 25 Hz in Fig. 7b [1]. This low coherence is responsible for the response we see in the test panel around its lowest resonances that will be discussed later.

The Optimized Reference SDM [13,14] that Jaguar's MIMO DFAT™ control uses, accounts for these facts by adjusting the shape of the relative coherence and phase, as a function of frequency, for the distance between microphones as well as other limitations of the acoustic testing facility that may exist, for which there is a patent pending [14]. As a result, the values we see for achieved coherence between microphones during MIMO DFAT™ testing are typically further reduced [14] than what we see from RATF testing, as we see in the following comparison shown in Figs. 8 and 9 (courtesy of Alan Merrick). Note that the relative coherence values in Fig. 8, from MSI-DFAT tests, are significantly lower below 1000 Hz, than those in Fig. 9 from RATF tests.

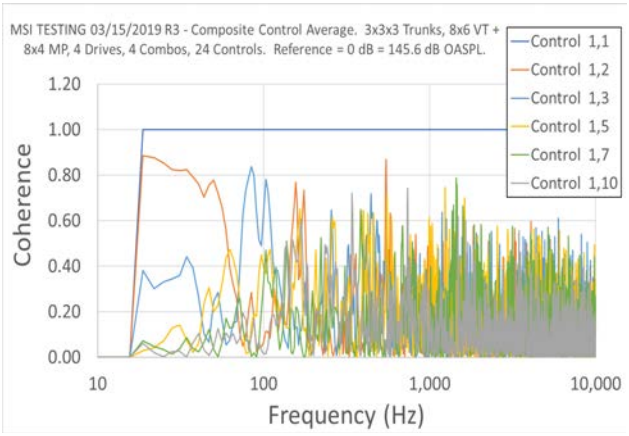

Fig. 8: Typical Relative Coherence MSI DFAT Results

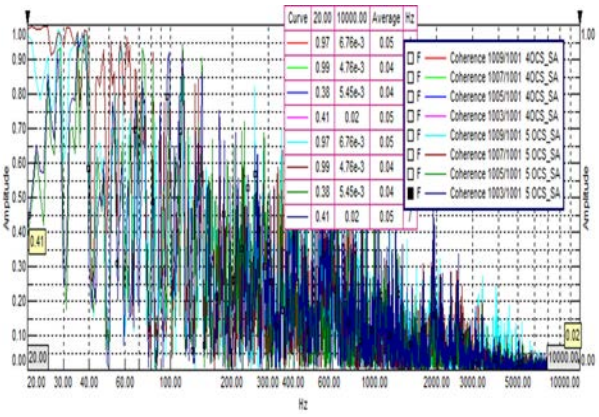

Fig. 9: Typical RATF Relative Coherence Results

e. Required Drive Signal Levels Needed for Test R5A

The largest drive used for Test R5A was seen to require a 0.276 Vrms signal. This value will be used as the dB reference to compare with the largest drive signals observed for the next three test results that will be discussed.

f. Panel Response PSDs

As discussed at the outset, the main objective of the described acoustic tests is to determine which acoustic field is best to use for acoustic tests, particularly those of significant structures like a Satellite and its components, by being

the best able to excite all the externally excitable structural resonances, which is expected to be a diffuse field as discussed in the section on coherence. Fig. 10 shows that this goal was achieved well by Test R5A, where the resonances identified by an independent Modal Analysis are found, sharply defined, and well excited.

Fig. 10 shows the response PSDs of 10 Accelerometers, between 35 Hz to 260 Hz, mounted on the panel during Test R5A, as shown in Figs. 2, 3 and 4. As can be seen, Fig. 10 identifies all 16 of the resonances, via the tagged cursors, that were found during the test, which correlate well with the16 damped resonances found by the subsequent Modal Test and Analysis that was performed, whose results are shown by Table 1 and Fig. 25. The resonance that was most difficult to find of the 16 that Modal Analysis identified, is the resonance at 203.1 Hz, which lies on the rising skirt of the resonance at 209.4 Hz that masks it, with only a slight peak visible. However, it can be better found as an obvious local maximum, by scanning the tabulated list of amplitudes of the PSD for various accelerometer for Test R5A, but not on similar data from the other three tests: R5B, R4A, and R5E. This fact and others will be discussed in more detail in a later section on the analysis of the individual PSD responses of the panel's 10 accelerometers, while comparing all 4 tests discussed in this paper for each individual accelerometer.

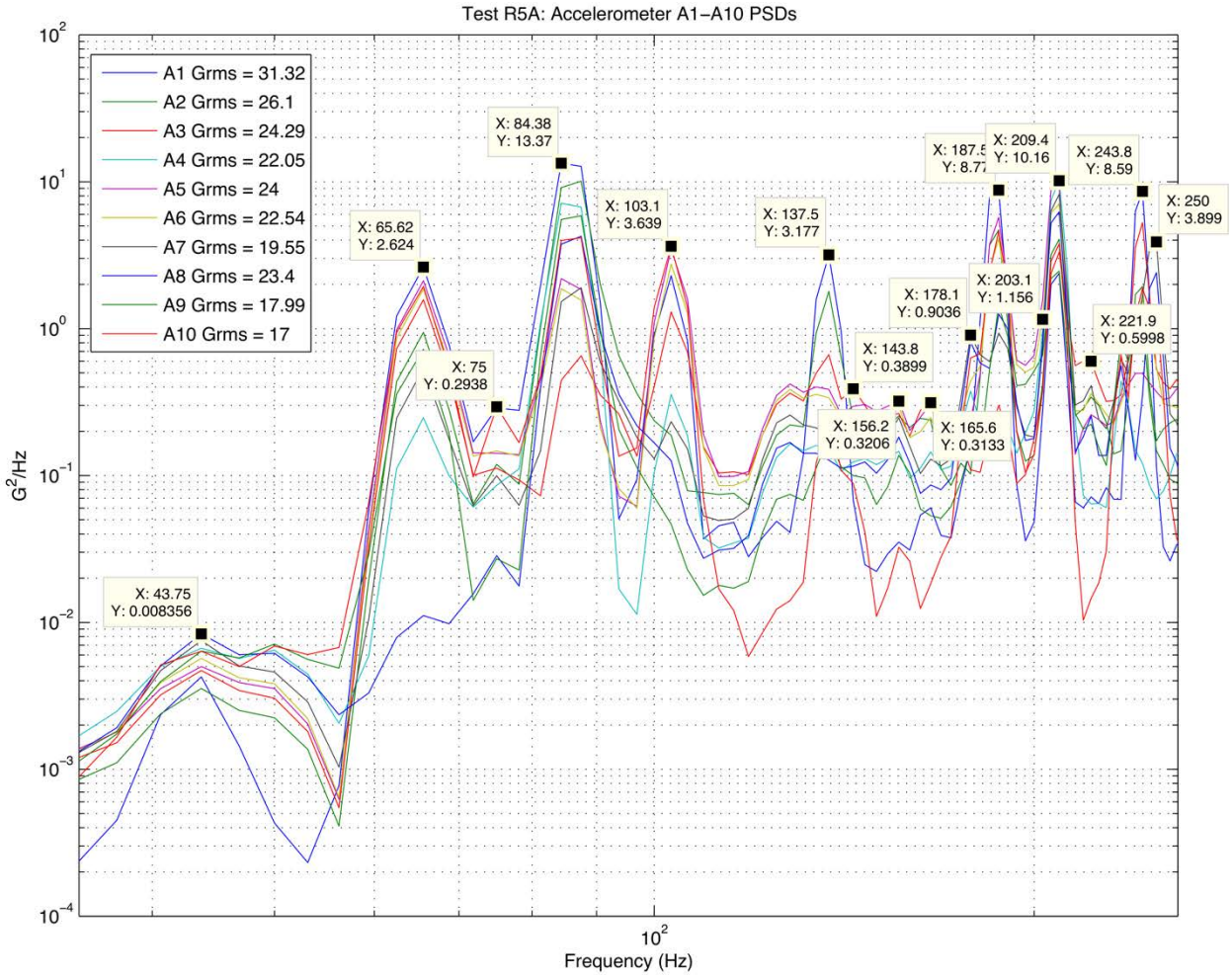

Fig. 10: PSDs of the Accelerometers mounted on Panel Plate During Test R5A

2. For test R5B the following results were obtained:

The following Fig. 11 shows good agreement between the average of all 24 control microphones and their reference for both 1/3rd Octave SPL and PSD spectra, but not as good as in Fig. 5 for Test R5A. Fig. 12 shows good control microphone PSD uniformity for Test R5B, but worse than what was seen for the diffuse Test R5A. Fig. 13a shows higher coherence between control microphone pairs [1, 2], through pairs [1,24] than what is seen in Fig. 7a for test R5A. Also, there is no longer the marked decline in coherence at 25 Hz that was seen and discussed for Fig.7a.

a. Average Control of the 24 Control Microphones as 1/3rd Octave SPL and PSD spectra

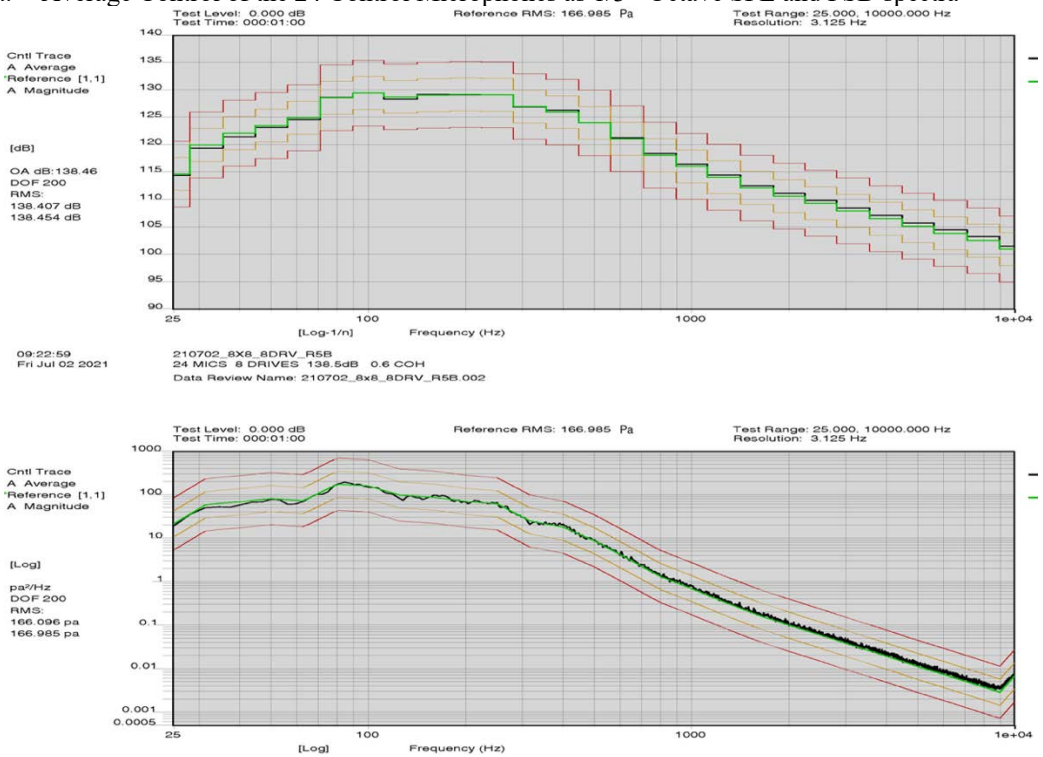

Fig. 11: Control Average as 1/3rd Octave SPL and PSD

b. Control PSDs, Coherence, and Phase

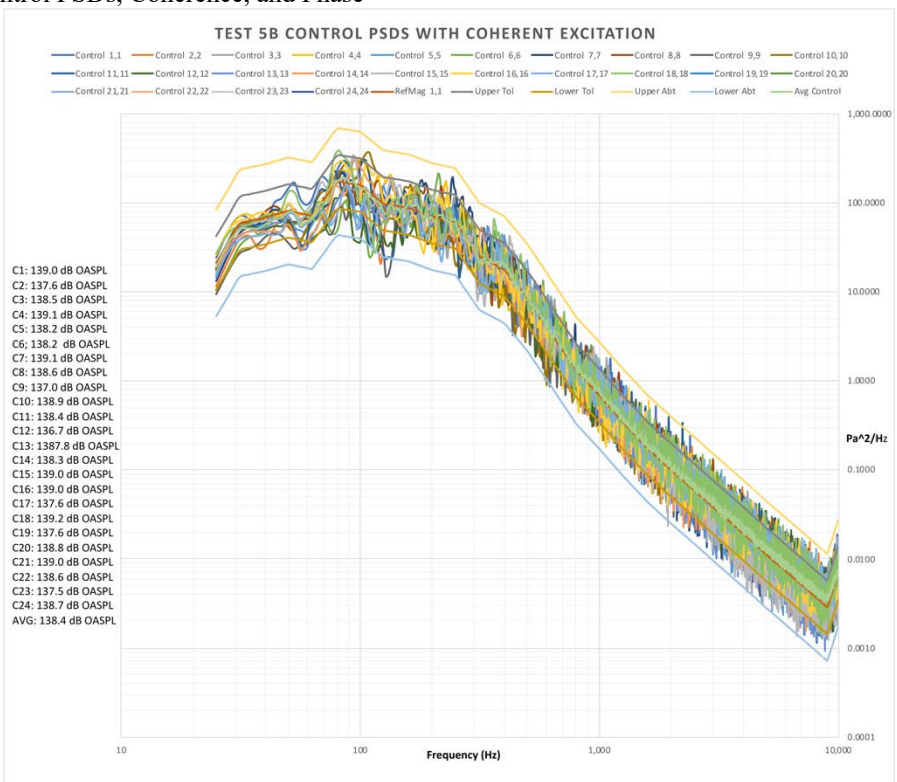

Fig. 12: Test R5B PSDs from 24 Control Microphone

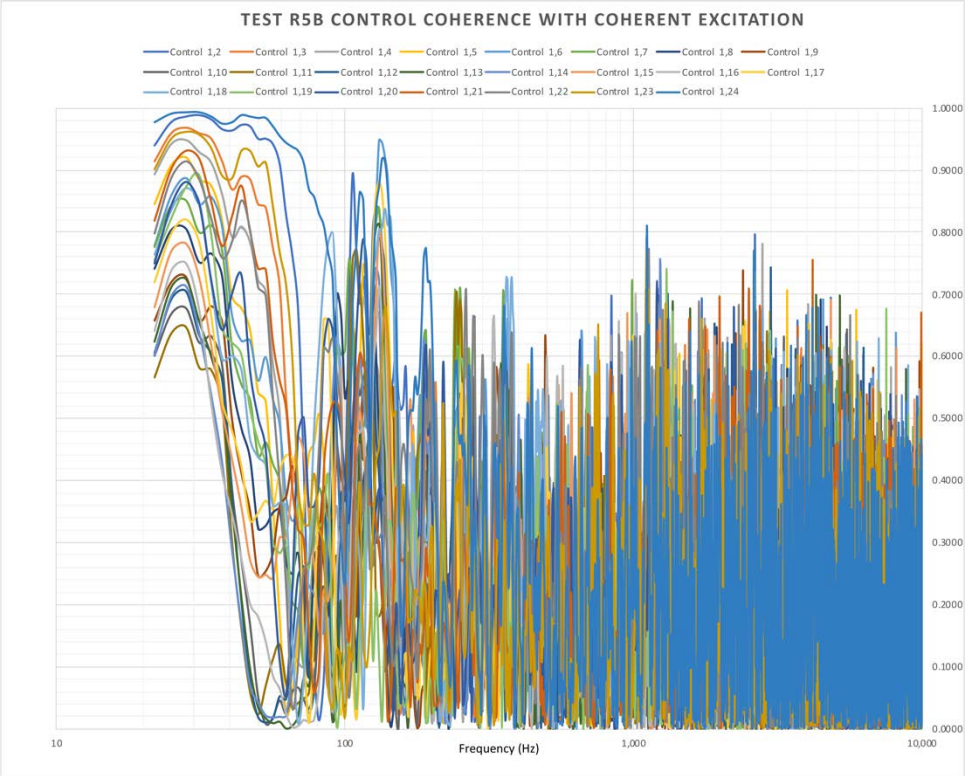

Fig. 13a: Test R5B Control Coherence from SDM top row

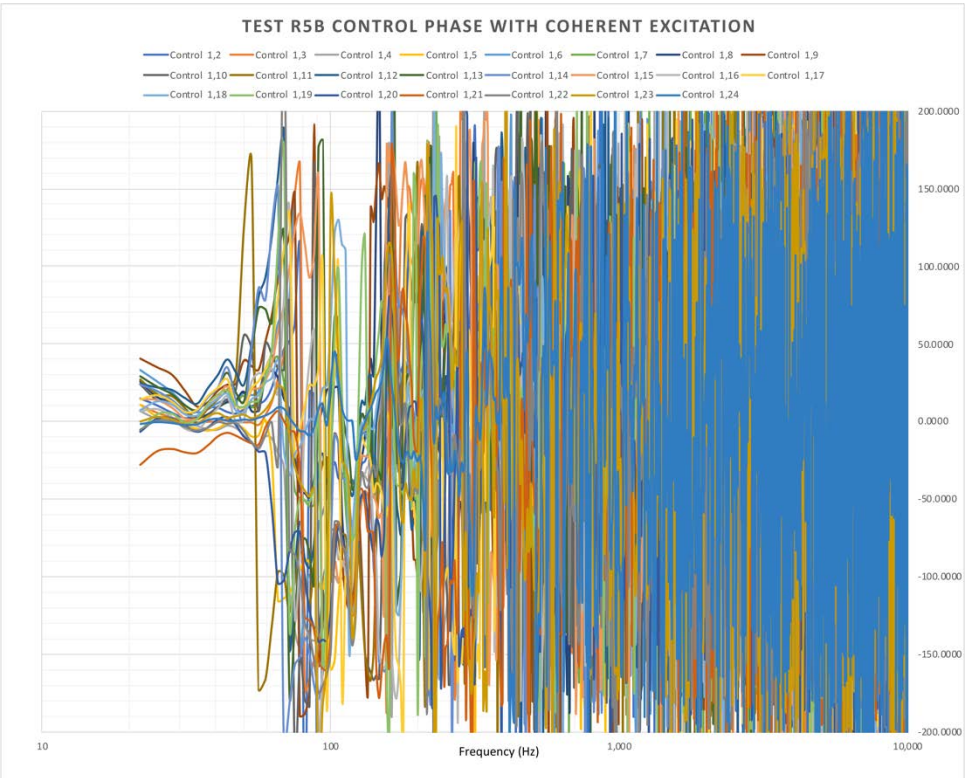

Fig. 13b: Test R5B Control Phase from SDM top row

For Test R5B, the goal of MIMO DFAT™ control is to keep the coherence high between microphones, but within what is physically possible, as shown by Fig. 13a. There is still a noticeable decline in control coherence seen in Fig. 13a below 100 Hz due to the increased distance between the control microphones, but not as severe as what was seen for Test R5A, due to the difference in the goal of MIMO control.

Fig. 13b shows near 0° relative phase between all microphones below 100 Hz and depending on their secant distance to nearly 150 Hz. Above 150 Hz, the phase becomes random due to the longer secant distances greater than ¼ wavelength as was discussed for Test R5A. This again demonstrates the dependence of the variance of the relative phase measurements as a function of the values of coherence. This higher coherence and the lack of random phase between microphones at the lower frequencies, as compared to what is seen for Test R5A, is what causes the test panel response differences with Test R5A that we will see in the next section.

Furthermore, these relative high values of coherence throughout the frequency range seen in Fig. 13a and the in-phase characteristics seen in Fig. 13b will be manifest in the response enhancement and cancellation effects, as a function of resonance phase, that will be seen in the panel response PSDs that will be discussed in conjunction with the following Fig. 14, which shows the panel response PSDs for all of the ten panel accelerometers for Test R5B.

c. Required Drive Signal Levels

For Test R5B it was noted that the largest drive now requires 0.282 Vrms, which is an increase of 0.187 dB over what was seen for the diffuse test results for Test R5A discussed previously.

d. Panel Response PSDs

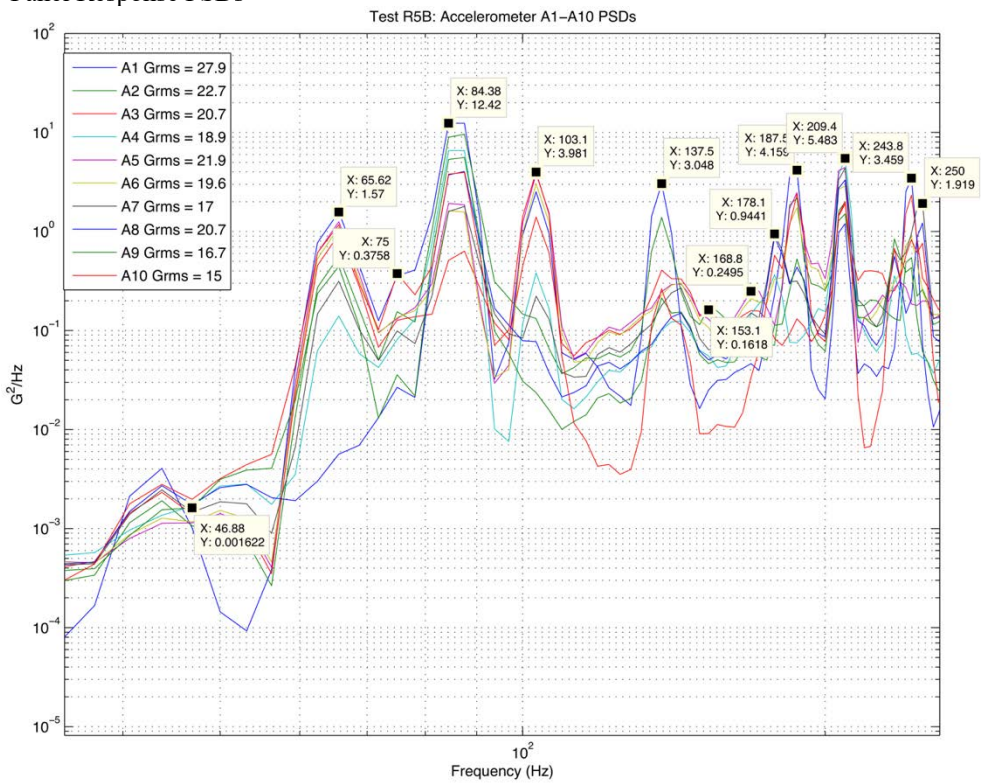

Fig. 14: PSDs of the Accelerometers mounted on Panel Plate During Test R5B

The previous Fig. 14 shows the PSD response of 10 Accelerometers mounted on the panel plate from Test R5B that is excited by a non-diffuse acoustic field with the same level and reference spectrum as for Test R5A, but with different relative coherence and phase characteristics discussed in the previous section. By comparing Fig. 14 with Fig. 10, several notable differences can be seen. For one, the peak Grms seen on the panel plate PSDs in Fig. 14, is now 21.9 Grms on A5, whereas in Fig. 10 it's on A1 at 31.3 Grms. Visually, Figs. 10 and 14 are significantly

different. In particular, the resonances in Fig. 14 are not as well defined or excited, as they are in Fig. 10, particularly below 260 Hz and very noticeably around the lowest resonance at 43.8 Hz and 75 Hz, and around 137.5 Hz, 156.2 Hz, and 165.6 Hz, where evidence of "phantom" resonances can be seen. The resonance at 43.8 Hz is missed by some accelerometers and the resonances at 143.8 Hz, 156.2 Hz, 165.6 Hz, and 221.9 Hz are missed.

Thus, evidence of response enhancement and cancellation is found, which is a result of the acoustic field being coherent and in phase for those frequencies, because of either the response or resonance phase being in phase or out-of-phase with the acoustic field excitation, or nearly so. The random phase and low coherence of the diffuse Test R5A for in this same frequency range, as shown by Figs. 7a and 7b, inhibit this effect from occurring, as can be seen by comparing Figs. 10 and 14. More examples of this type of effect will also be seen in the following non-diffuse test results: directed coherent acoustic field Test R4A and MISO Test R5E to be discussed.

The response enhancement and cancellation effects from using a non-diffuse acoustic test, will be further discussed in more detail in conjunction with the analysis of the panel response as a function of Tests: R5A, R5B, R5E, and R4A for each of the 10 response Accelerometer PSDs in the later section V of this paper.

3. For test R4A the following results were obtained:

   a. Average Control of the 24 Control Microphones as 1/3rd Octave SPL and PSD spectra

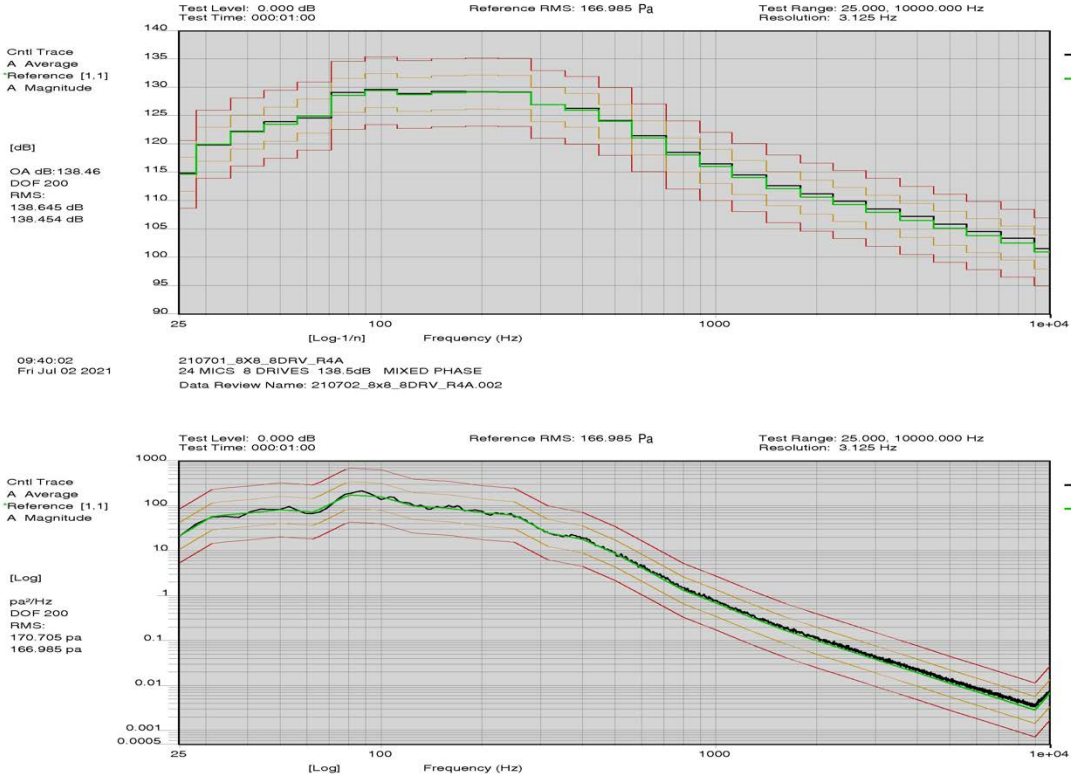

Fig. 15: Control Average as 1/3rd Octave SPL and PSD

As has been seen for Test R5B the average control displayed by Fig. 15 for Test R4A, shows good agreement between the average of all 24 control microphones and their reference for both 1/3rd Octave SPL and PSD spectra, but slightly worse than what was seen for Test R5B. Fig. 16 shows good control microphone PSD uniformity, which is slightly better than what was seen for the high coherence (non-diffuse) acoustic field test R5B.

   b. Control PSDs, Coherence, and Phase

We will discuss only some relative coherence results between control microphones, for Test R4A, since this subject is more complex than what we've seen for Tests R5A and R5B. Relative coherence and phase between control

microphones needs to be organized into 3 groups, for which the nominal relative coherence is set to 0.7, within each group: 1) above (top) the test panel (as shown in Fig.1b); 2) below (bottom) the test panel; and 3) to the right and left of the test panel, as well as between groups, where all three groups of control microphones can be seen by examining Fig. 1b. We also now need to be concerned with the relative phase between control microphones at a higher level of detail and with more care, since the resulting reference SDM must be positive definite and poor choices for the relative phase will result in non-positive SDMs that are not feasible.

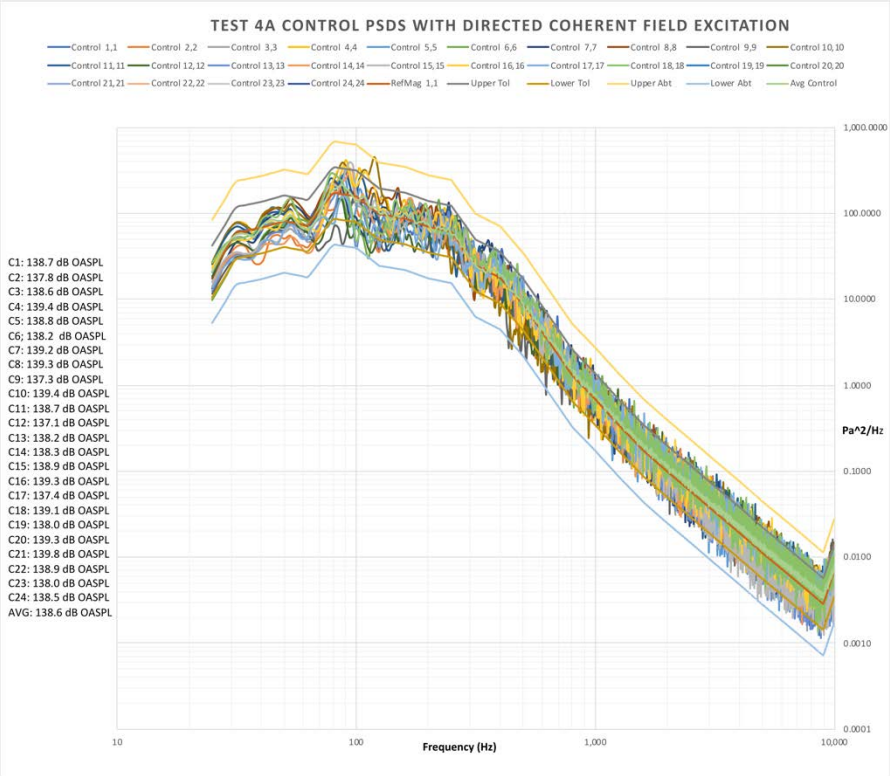

Fig. 16: Test R4A PSDs from 24 Control Microphone

Since the objective of Test R4A is to create a directed coherent acoustic field to excite the panel, we need to be concerned with high coherence, 0.7, between all of the control microphones as in Test R5B, which was nominally set to be 0.6, but now will have to be additionally concerned with the relative phase between the control microphones within and between the same three groups as for relative coherence, but in a more complex manner. There are also diffraction effects caused by the directed coherent field approaching and leaving the test panel at its front and rear, which affects the settings of phase and coherence between groups. But since the focus of this paper is the response of the test panel excited by diffuse, non-diffuse, and MISO control created acoustic fields, we will only discuss the top and bottom control microphone groups with regards to the relative coherence and phase within each microphone group, as can be seen in Fig. 1b, to give the reader an introduction to some of the issues associated with directed coherent acoustic field testing.

Fig. 17 shows the relative coherence between the control microphone pairs within the top group of microphone pairs: [1,18] through [1,24], [18,19] through [18,24], [19,20] through [19,24], [20,21] through [20,24], [21,22] through [21,24], [22,23] through [22,24], and [23,24]. Note that they're nearly one for frequencies below 100 Hz, which as can be seen as close to or above the nominal target of 0.7, whose indices correspond to the control microphone numbers that are shown in Fig. 1b.

Also, there is no marked decline in coherence at 25 Hz as seen and discussed for Fig.7a, since the goal of MIMO DFAT™ control is to keep the coherence at or above 0.7 between microphones, as was seen for Test R5B at the lower target of 0.6, but within what is physically possible. There is still a decline in control coherence above 100 Hz,

to a nominal value of 0.7, but with much variance, as seen in Fig. 16, but at a higher nominal level, due to the higher setting of the relative coherence, as compared to the 0.6 that was set for Test R5B.

The high variance we see above 100 Hz is probably because at the higher frequencies, the wavelengths are much shorter, and that the coherence is difficult to be kept high as the distance between microphones increases, as we also see for Test R5B. Despite those difficulties, Fig. 17 shows that the nominal relative coherence is higher than what was seen for that Test R5B.

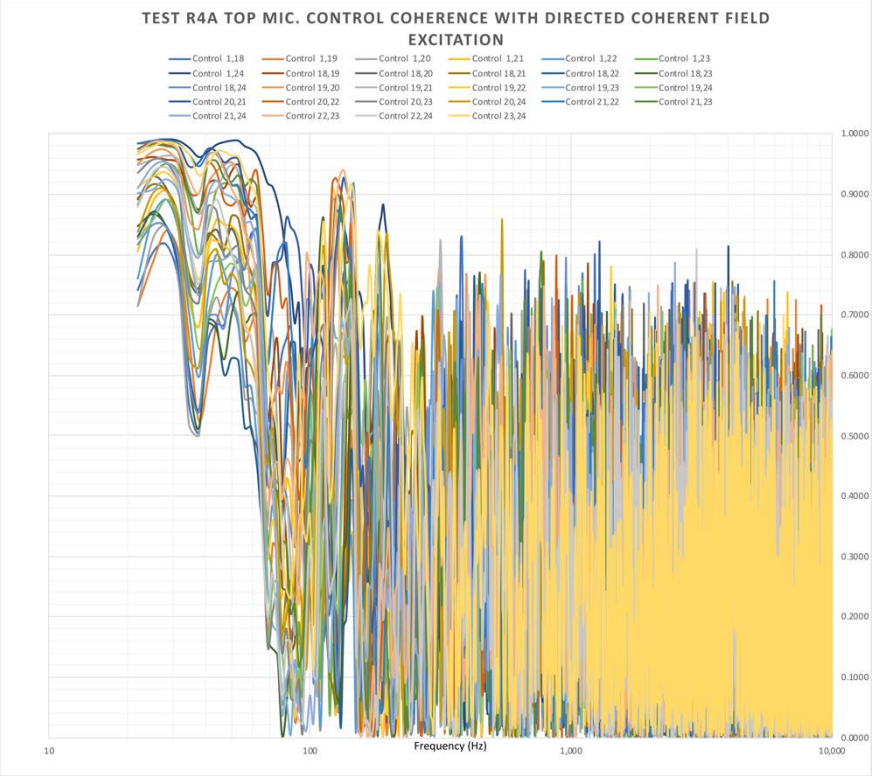

Fig. 17: Test R4A Top Control Microphone Relative Coherence

Fig. 18 shows the corresponding relative phase for the same group of control microphones that demonstrates that the relative phase below 100 Hz was kept by MIMO control near 0^{o} as nominally set. Above 100 Hz, the phase become more random, due to the difficulties in keeping the coherence consistently at or above 0.7. Phase randomly becomes low above 100 Hz as Fig. 18 shows, which further indicates that it's due to the diffraction effects of the test panel negatively affecting the measurement of coherence. On a practical level, the fact that phase becomes more random above 100 Hz, for some microphone pairs, may mean that the directed coherent field we generate, may only be effective below 100 Hz, which is well within the expectations we had for Test R4A. However, other analyses of the coherence and phase within and between groups shows that the directed coherent field appears to be effective to 144 Hz, which is better than we expected and more than adequate for our structural response evaluation, since the most significant test panel plate modes are those below 144 Hz, as will be discussed in the following sections. However, a final determination will have to wait till then, before being more conclusive.

Fig. 19 shows the relative coherence between the bottom control microphones pairs: [6,13], [7,8] through [7,13], [8, 9] through [8,13], [9,10] through [9,13], [10,11] through [10,13], [11,12] through [11,13], and [12,13]. Note that they're mostly close to one for frequencies below 100 Hz, with a few below the nominal target of 0.7, where except for one trace, all above 0.4. That trace corresponds to the relative coherence between bottom control microphones 6 and 13, i.e., from the right end of the panel to the other end due to diffraction, which is not surprising.

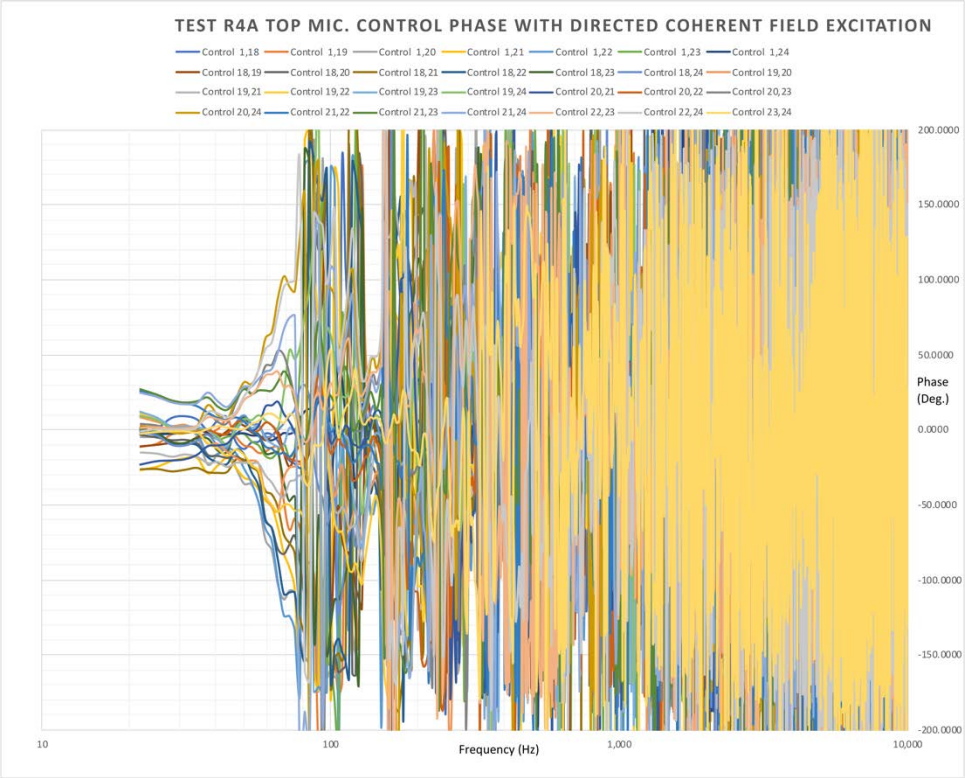

Fig. 18: Test R4A Top Control Microphone Relative Phase

Fig. 19 also shows, as for the top control microphone group, that the nominal coherence between those control microphones is again close to the nominal target of 0.7 above 100 Hz. This again fully supports the view that the directed coherent field excitation, which is superimposed on a nominal 30% diffuse acoustic field, should excite the panel well below 100 Hz, which is within our expectations for Test R4A, but where this view will be more critically examined during the detailed panel response analysis in the later section V, since other coherence and phase analyses, which won't be discussed further in this paper due to the increase in scope that this would require, indicate that the directed coherent field excitation is actually effective to frequencies as high as 144 Hz.

The view that the directed coherent field is effective below 100 Hz is further supported by Fig. 20, which shows that the relative phase between all of the bottom control microphones is close to 0° below 100 Hz. This means that both the top and bottom speakers are nearly in phase within each group below 100 Hz and that there will be a directed coherent field excitation superimposed on a nominal 30% of diffuse acoustic field content for at least those frequencies.

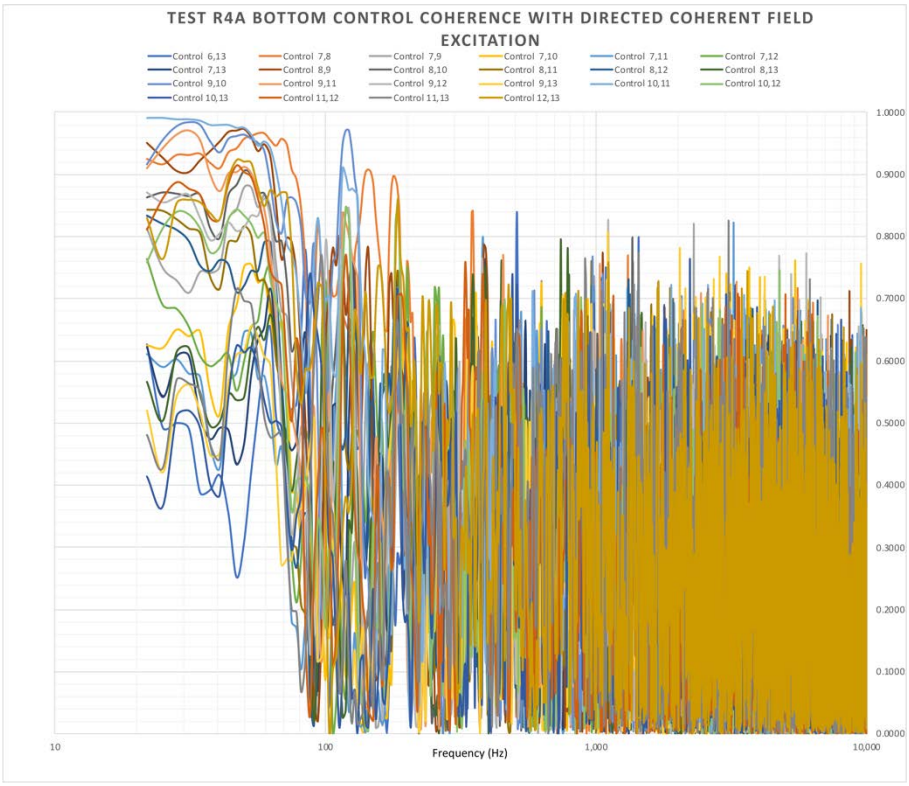

Fig. 19: Test R4A Bottom Control Microphone Relative Coherence

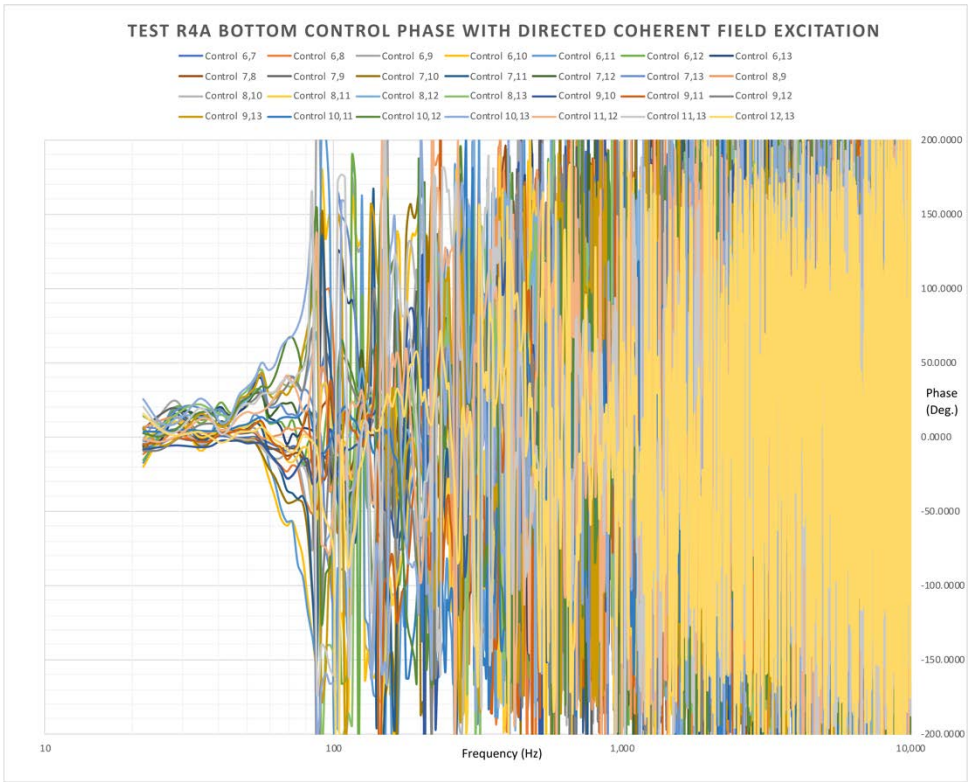

Fig. 20: Test R4A Bottom Control Microphone Relative Phase

As we saw for the top group of control microphones, we also have that the phase becomes random above 100 Hz for some of the bottom microphone pairs, as shown by Fig. 20, probably for the same reasons that were given for the top group's phase response above 100 Hz, which again appear to be due to the diffraction of the directed coherent field as it reaches and leaves the test panel, which further negatively impacts the measurement of coherence and phase.

However, since we have high coherence between microphones within each top and bottom group, those results do support the view that at the very least that we have two independent directed coherent fields excitations for the top and bottom surfaces of the test panel, as shown in Fig. 1b, from 25 Hz to 100 Hz, but possibly to the higher frequencies between 100 Hz and 144 Hz.

This view is supported by the other analyses that have been performed. It indicates that the diffraction effect we've discussed only obscures, by lowering the coherence between and within the top and bottom microphone groups but may not prevent the effectiveness of the directed coherent field for the higher frequencies. This conjecture appears to be true, since this explains and is consistent with why we see resonance cancelling and enhancement effects in the response of the panel's accelerometer PSDs to Test R4A's excitation over a larger range of frequencies that is seen and discussed later, both in the following sections d and V, where these panel response results are analyzed.

Those directed coherent acoustic field wave fronts, in front and behind the test panel that these coherence and phase results imply exist, have similar characteristics to standing waves [3,12,13], but for a broader range of frequencies and over broader areas. We'll see in the following section d and V evidence to support that view, where we'll see response enhancement effects, as we've seen for the test results from Test R5B, but for a broader range of frequencies and over more of the panel's acceleration PSD responses, as expected.

c. Required Drive Signal Levels

The largest drive for Test R4A required 0.279 Vrms, which is a slight increase of 0.09 dB from what was seen for the diffuse Test R5A, but slightly less than what occurred for the non-diffuse test R5B, i.e. 0.09 dB less. Additionally, it requires 1.9 dB more drive than the MISO Test R5E.

d. Panel Response PSDs

The following Fig. 21 shows the PSD response of 10 Accelerometers mounted on the panel plate from Test R4A, excited by a non-diffuse directed coherent acoustic field at the same level and using the same reference spectrum, as in the previous tests. By comparing Fig. 21 with Fig. 10, several notable differences can be seen. For one, the peak Grms seen on the panel plate PSDs in Fig. 21 are now 33.2 Grms on A1, whereas in Fig. 10 it's on A1 but at 31.3 Grms. Visually, Figs. 10 and 24 are significantly different, particularly for the frequencies surrounding the resonances at 43.8 Hz, 75 Hz, 84.4 Hz, 103.1 Hz, 134.7 Hz, and at 209.4 Hz, which is like what we saw for Test R5B, but more concerning. For test R4A, significant side lobes appear around 43.8 Hz, 75 Hz, 103.1 Hz, and around 134.7 Hz, on the order of the magnitude of the resonance at that frequency. The response at 134.7 Hz for Test R4A is significantly lower than on all accelerometers response we've seen for Test R5A and even on those for Test R5B. Some accelerometers show evidence of what appears to be complete response cancellation of the 134.7 Hz resonance, which is consistent with a directed coherent field to 144 Hz, as was explained at the end of section b, which will be further discussed in the later section V. Additionally, the response at other resonances is higher than seen for other tests, i.e. evidence of response enhancement, but where the response between 103.1 Hz and 187.5 Hz is significantly lower, i.e. partial response cancellation, like what has been discussed previously.

Fig. 21 also shows evidence of "phantom" resonances at 40.6 Hz, 53.1 Hz, 128 Hz, and 159.4 Hz. The Resonances at 43.8 Hz, 75 Hz (by most accelerometers), 156.2 Hz, 165.6 Hz, 203.1 Hz, and 221 Hz are totally missed by Test R4A, as shown by Fig. 21. These provide further evidence of response or resonance enhancement and cancellation because of using the highly coherent and directional non-diffuse field provided by Test R4A.

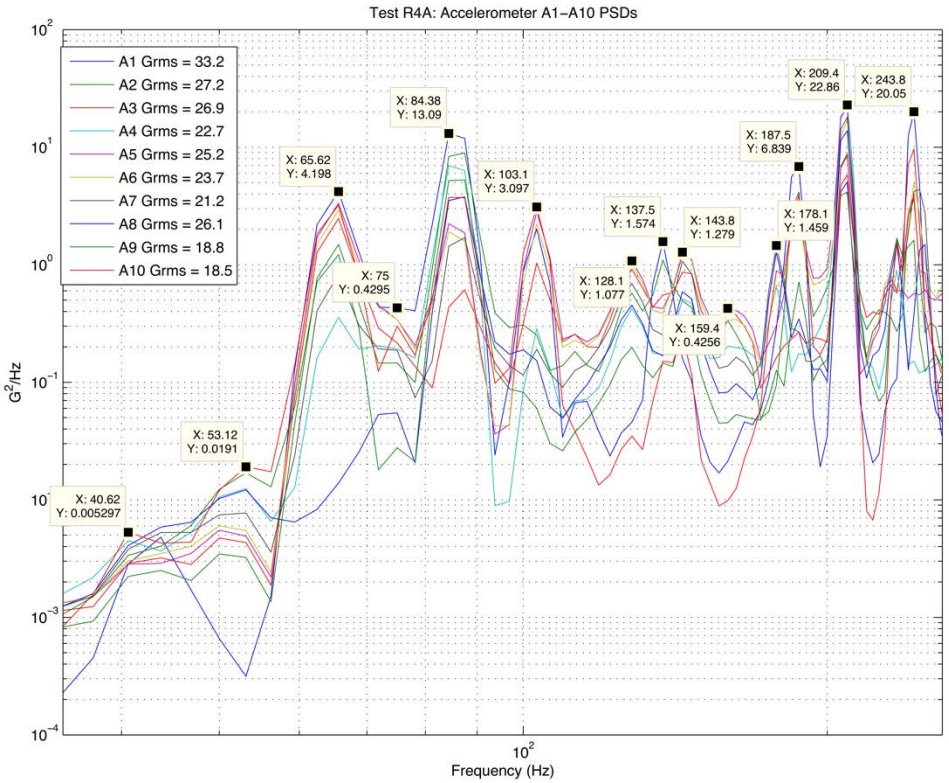

Fig. 21: The PSDs of the Accelerometers mounted on Panel Plate During Test R4A

4. For test R5E the following results were obtained:

   a. Average 1/3rd Octave SPL and PSD spectra and individual 24 control PSDs

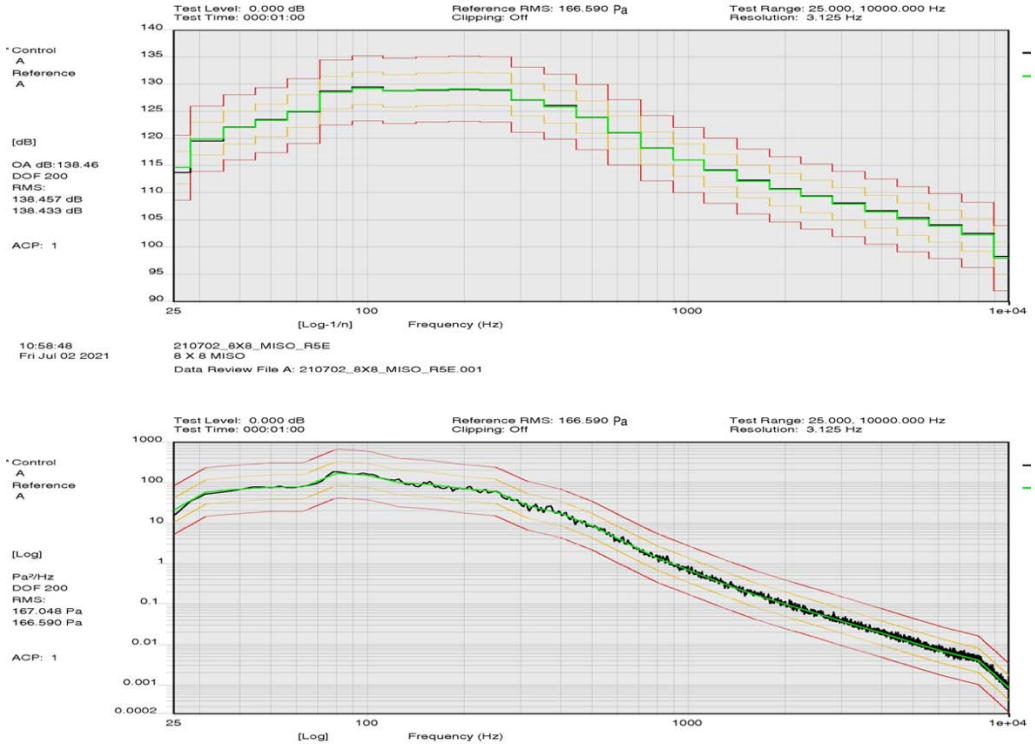

Fig. 22: Control Average as 1/3rd Octave SPL and PSD

The average control displayed by the previous Fig. 22 for Test R5E, shows good agreement between the average of all 24 control microphones and their reference for both 1/3rd Octave SPL and PSD spectra, but not as good as for Tests R5A, R5B, and R4A. Unfortunately, the graph in Fig. 22 is misleading, but the typical manner MISO [4,12] acoustic test results are reported, such as for Test R5E, which obscure the underlying problems [12-14] associated with MISO acoustic testing, since it does not give a complete or accurate picture of how the acoustic field behaves.

One underlying problem is made clear by examining the individual control microphone PSD responses displayed by Fig. 23a. The most notable differences between Fig. 23a, and Figs. 6, 12, and 16 is the poorer control microphone PSD uniformity from MISO as compared to MIMO control. This is not surprising, since MISO control has no provisions to control the individual response of control microphones and the response of acoustic modes that MIMO control has [4,12-14]. In effect the response at every microphone response is totally dependent on the factors discussed for MISO controllers in the next paragraphs and in [4,14], i.e., there is no coherence or phase control capability for MISO tests. A result of this fact for MISO Test R5E is manifested by the peak to valley spread shown by Fig. 23a in PSD response, which is on the order of 25 dB as compared to the less than 3 dB we see for Test R5A. This is not the worst, since we've seen worse PSD spreads in other MISO DFAT™ tests [4,12,13]. In this case, most of the spread is due to the dips and high peaks we see in the PSDs for control microphones around 300 Hz.

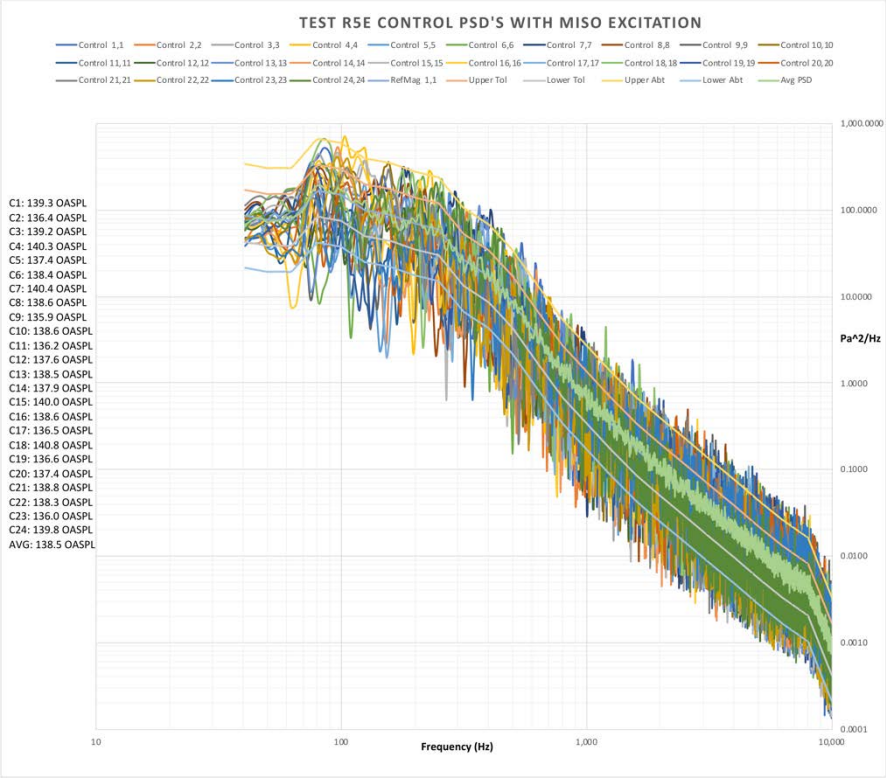

Fig. 23a: Test R5E 24 Control Microphones PSDs

b. MISO coherence and phase

For the MISO Test R5E, Fig. 23b shows that the coherence between control microphones is nearly 1 for the entire frequency range. Fig. 23c shows the phase between control microphones is nearly zero with a slowly increasing phase shift due to the time delay between microphone responses. The result is a highly non-diffuse acoustic field, since the coherence and phase spectra between control microphones is not being controlled and the control coherence and phase spectra obtained are totally dependent on the acoustic modal structure of the test room volume, the speaker configuration, the microphone configuration, and the interaction with the test article, where all of which can vary considerably between different tests. Thus the character (the variation between microphone responses and their relative coherence and phase) of this non-diffuse field can change significantly test to test, which is typical.

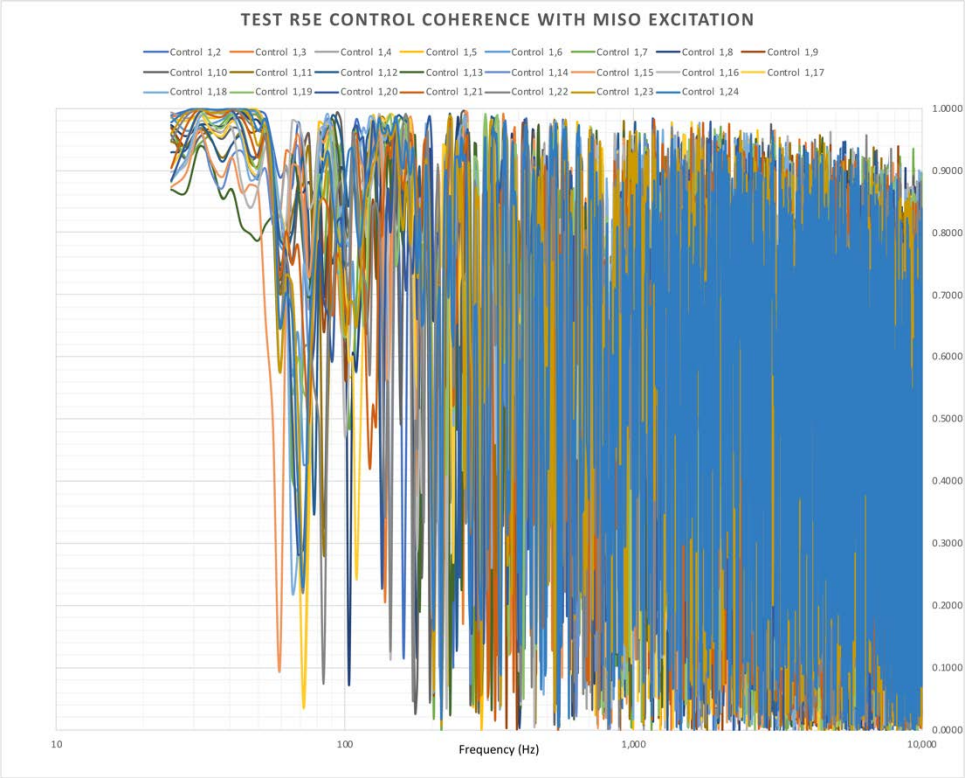

Fig. 23b: Test R5E 24 Control Coherence Between Microphone Responses

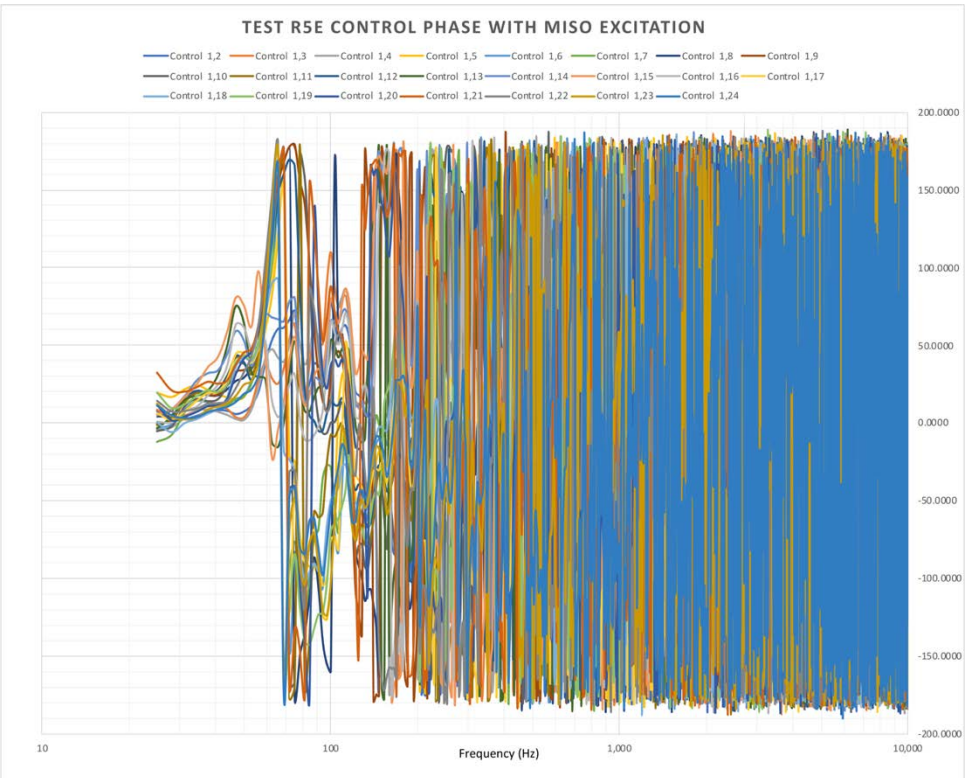

Fig. 23c: Test R5E 24 Control Phase Between Microphone Responses

Additionally, standing waves may be present in the achieved acoustic field [3,4,12-14], since there are no provisions for their control [12,13], which can cause severe over-testing when their frequencies and phase responses at high coherence coincide with structural resonance frequencies, as has been reported [3,4,12,13], which is a form of response enhancement that occurs when the acoustic field spectral content coincides in phase at high coherence with the resonant behavior of the structure under test [3,4] and a cause of structural "hot spots" during an acoustic test [3,4]. Response cancellation can also occur when the acoustic field's standing wave or modal response spectral content is out-of-phase at high coherence with the resonant behavior. Both effects occur with all non-diffuse acoustic field excitations, but worse for MISO testing due to their coherence and phase characteristics, as will be seen later during the analysis of response to the various acoustic fields, for the three non-diffuse tests discussed.

This control behavior is typical of all MISO control [4,12] implementations, even for the extended MISO controllers discussed in [14], that use multiple conventional MISO controllers independently operating in tandem (some of which within a single control system, which is a weak form of MIMO control), with each controller having a MISO controlled output based on the average response of selected subsets of control microphones, all exciting the same acoustic field (or system) [14]. These controllers also don't have an ability to control the overall acoustic field response, like the acoustic modes that may exist in the acoustic field, since they don't have the ability to control the cross-coupling effects that result from exciting any dynamic system with multiple drives and not effective MIMO controllers, as discussed in 6.3.3 of [4]. This is exacerbated by the fact that some don't have provisions for narrow-band control, but rather their control is based on "equalizing" the response of band-pass n^{th} octave filters, which lacks the higher resolution control that Test R5E has, as described by the promotional literature for those types of systems. These extended MISO systems are essentially multiple SISO [4] controllers exciting a single acoustic field that don't have the ability to control the off-diagonal elements of the resulting SDM response and thus can't uniquely control the response of each control microphone [11-13].

e. Required Drive Signal Levels

The signal level of the drive for MISO Test R5E is 0.224 Vrms, which is lower than the diffuse MIMO Test R5A, but by only -1.81 dB and -2.00 dB less than the non-diffuse MIMO Test R5B. Note that the 1.81 dB power penalty of MIMO over MISO is lower than otherwise reported by others in their promotional literature.

c. Panel Response PSDs

Fig. 24 shows the PSD response of the same 10 Accelerometers mounted on the panel plate that have been discussed for Tests R5A, R5B, and R4A, but which are now shown for the MISO Test R5E, which is also excited by a non-diffuse acoustic field that's uncontrollably so and at the same level and using the same reference spectrum as those previous tests. By comparing Fig. 24 with Fig. 10, many of the same notable differences we saw between Fig. 10, Fig. 14, and Fig. 21 can also be seen in Fig. 24, but in a worse manner.

The peak Grms seen on the panel plate PSDs in Fig. 24, is now 28.3 Grms on A1, whereas in Fig. 10 it is A1 at 31.3 Grms, in Fig. 14 it is A1 at 27.9 Grms, and in Fig. 21 it is 33.2 Grms on A1. The panel response for Test R5E is also different from what we see for the other tests in that it's dominated by the PSD for A1 at an apparent resonance at 366 Hz (not shown if Fig. 24), which doesn't appear in any of the other panel responses or in the Modal Analysis results.

But more concerning, the resonance behavior is completely different from what we see in Figs. 10, 14, and 21, i.e., more poorly defined and excited modes, particularly when compared to the results shown in Fig. 10, e.g. at 43.8 Hz, 65.6 Hz, 75 Hz, 84.4 Hz, 103.1 Hz, 137.5 Hz, 156.2 Hz, 165.6 Hz, 178.1 Hz, 203.1 Hz, 221.9 Hz, and 243.8 Hz, which again show the resonance response effects that have been discussed for non-diffuse fields. In fact, the resonances at 137.5 Hz, 156.2 Hz, 165.6 Hz, 178.1 Hz, 203.1 Hz, 221.9 Hz, and 243.8 Hz are totally missed. Most resonances are also under excited.

Visually, Fig. 24 shows more significant difference between Figs. 10 and 14 in other areas, particularly the area between 103 Hz and 187 Hz, where the mode at 137.5 Hz is entirely missed. More concerning are the "phantom" resonances are seen around 43.8 Hz, 65.6 Hz, 75 Hz, 85.4 Hz, 103.1 Hz, 137.5 Hz, 156.2 Hz, 165.6 Hz, and 178.1 Hz on various accelerometers. This implies that MISO is the poorest test method, as compared to tests R5A, R5B,

and R4A for exciting structural resonances, but with strong similarities to Tests R5B and R4A, with respect to its response effects on the test article. Again, this subject will be discussed later in more detail.

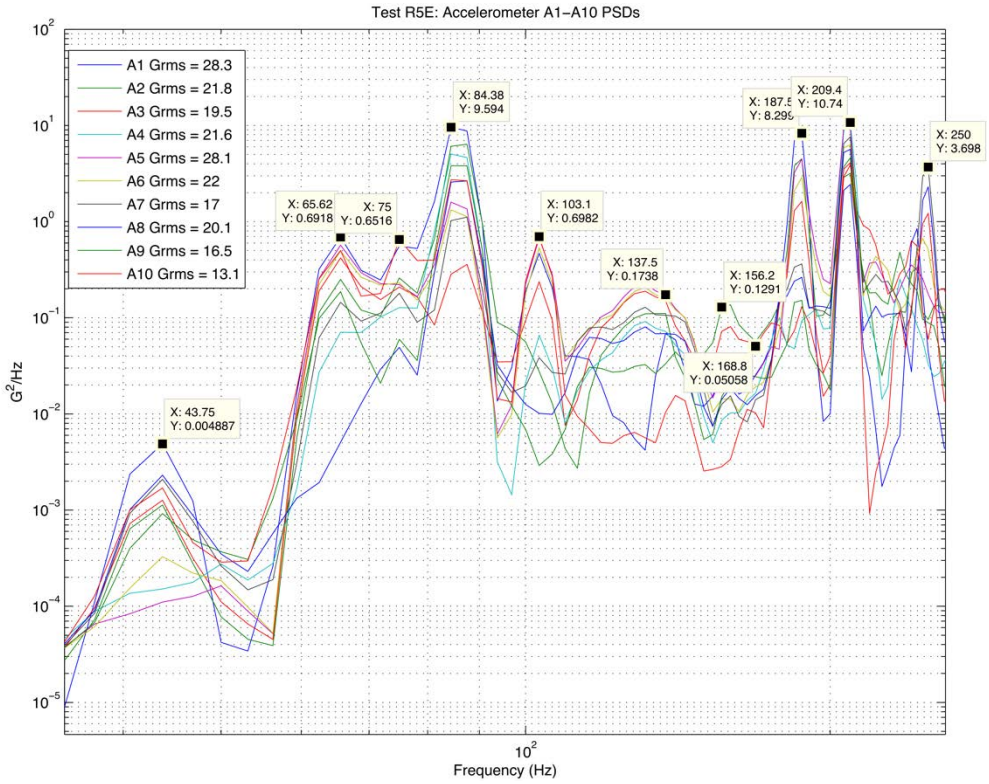

Fig. 24: PSDs of the Accelerometers mounted on Panel Plate During Test R5E

V. Detailed Examination of Accelerometer Responses from Tests R5A, R5B, R5E, and R4A

1. Modal Testing and Analysis Results

A series of Modal Tests were performed after the Acoustic Tests were completed, to gather data to determine the modes of vibration of the panel that was tested. Figure 2 shows a photo of the panel and placement of the 10 Accelerometers that were used for that purpose, A1 through A10, that have been discussed in previous sections. The 45 points that were excited by hammer blows are also shown in Figure 2 numbered 0-44, as has been discussed.

Frequency Response Functions (FRFs) were measured between each of the 45 excitation points and the 10 measurement accelerometers that are shown in Fig. 2, 3, and 4. The coordinates and placements of the 10 response accelerometers are also shown in those figures. These measured FRFs were then analyzed by Star Modal™ to determine the first 25 modes below 400 Hz. Their natural frequencies, damping, and damped frequencies are shown in Table 1, for first 16 modes, which are the ones discussed in this paper, since the most significant potential stress/strains are seen with the lower frequency modes, as a result of their larger structural deflections. The Observed Resonant Frequency column was determined by examining the PSD spectra of the accelerometers mounted on the panel, A1 through A10, as shown in Fig. 10 for Test R5A, for isolated peaks and correlating them with the Damped Resonant Frequency column, which takes the damping effects on the mode's natural frequency into account, i.e., it lowers its frequency accordingly. Only the diffuse Test R5A properly excited all of the 16 expected resonances.

Fig. 25 shows the mode shapes corresponding to the first 16 modes that were identified by Modal Analysis. They are shown in a grid format consisting of four blocks, where each block contains four mode shapes, with the lowest frequency mode shape on top and highest frequency mode shape at the bottom of the block. Fig. 25's contents, as

identified in Table 1, are as follows: 1) the upper left block contains modes 1-4; 2) the upper right block contains modes 5-8; 3) the lower left block contains modes 9-12; and 4) the lower right block contains modes 13-16.

Table 1: Modal Analysis Frequencies Comparison with Observed Resonant Frequencies

Mode	Natural Frequency (Hz)	Damping Ratio (Hz)	Damping Ratio (%)	Damped Resonant Frequency (Hz)	Observed Resonant Frequency (Hz)	Observation Discrepancy (%)
1	43.77	2.46	5.62	43.70	43.8	0.23
2	69.32	0.18	0.26	69.32	65.6	-5.37
3	77.72	1.02	1.31	77.71	75.0	-3.49
4	85.65	20.04	22.78	83.40	84.4	1.20
5	103.43	7.39	7.13	103.17	103.1	-0.06
6	131.13	1.31	1	131.12	137.5	4.86
7	143.71	0.08	0.05	143.71	143.8	0.06
8	153.59	2.17	1.41	153.57	156.2	1.71
9	172.76	1.07	0.62	172.76	165.6	-4.14
10	181.35	0.51	0.28	181.35	178.1	-1.79
11	187.51	0.58	0.31	187.51	187.5	-0.00
12	202.42	1.3	0.64	202.42	203.1	0.34
13	208.97	0.61	0.29	208.97	209.4	0.21
14	222.36	1.84	0.83	222.35	221.9	-0.20
15	240.07	1.1	0.46	240.07	243.8	1.55
16	247.94	0.64	0.26	247.94	250	0.83

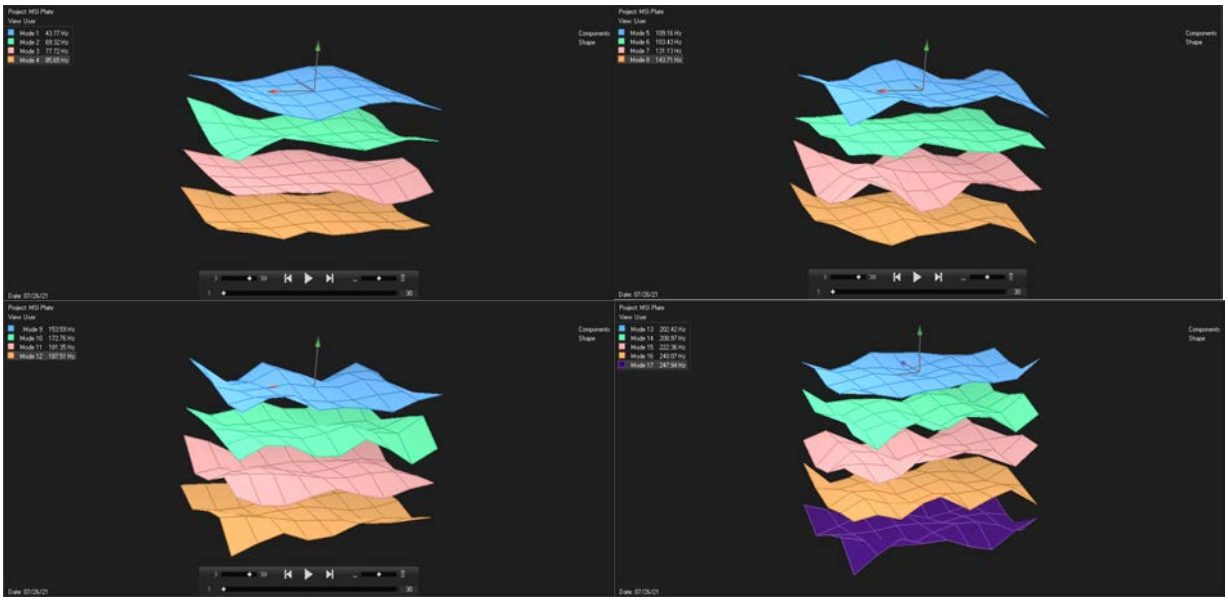

Fig. 25: The first 16 Mode Shapes Described by Table 1

In the following section 2, each of the 4 test's response PSDs, for each of the 10 panel accelerometers, will be compared to each other to see how well tests are able to identify the damped frequencies of the 16 modes listed in

Table 1, by the resonant peaks they show during each of the 4 tests. Notice that the Damped Resonances and Observed Resonances don't always agree. Much of this is due to the lower frequency resolution used for the acoustic test, 3.125 Hz, whereas Modal Analysis used a higher resolution as a result of its internal interpolation capability. However, the amount of discrepancy match seen in the results listed in Table 1 is consistent with the experimental variations that typically occur between testing and Modal Analysis results.

The panel response PSDs for each accelerometer, from each of the four types of tests, will also be compared on how well the 16 modes were excited, in the section that follows. All plots of panel PSDs in this paper, including Figs. 10, 14, 21, 24, and those that follow are displayed using the expanded range between 35 Hz to 260 Hz.

2. Response PSDs for A1 and A2 as a function of Tests R5A, R5B, R4A, and R5E

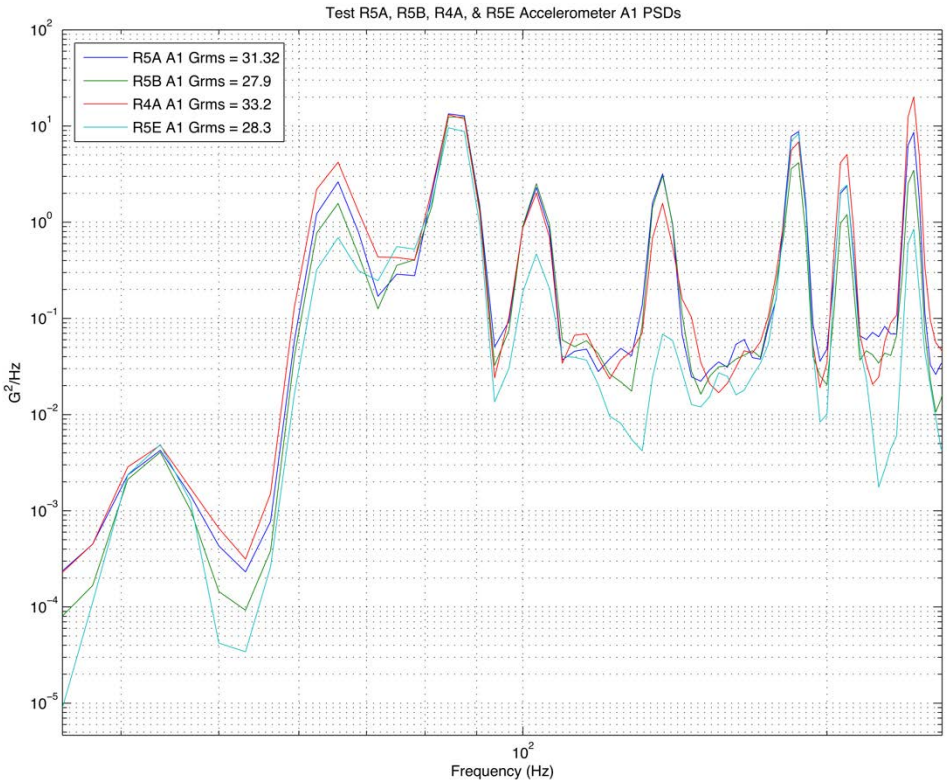

Fig. 26: A1 PSD Comparison for Tests R5A, R5B, R4A, and R5E

Note how well the incoherent MIMO DFAT™ test R5A sharply defines all of the structural resonances seen by Accelerometers A1 and A2, particularly the first 16 modes, as well as the mode at 137.5 Hz shown in Figs. 26 and 27. Note that only test R5A defines the modes below 200 Hz very well in Fig. 27. Test R4A and R5E are the worst in this regard, where Test R5E misses adequately exciting the resonance at 137.4 Hz entirely and Test R4A either over or under excites most modes. Side lobes are evident in R4A's response around 137.4 Hz, as well as in Test R5E's response in Fig. 27, where "phantom" resonances appear for both, where both appear to be examples of response enhancement and cancellation, as has been discussed. The resonance at 43.8 Hz is only correctly defined in Fig. 27 by test R5A, whereas Test R4A shows significant sidelobes, and which is the most significant structural resonance, since it has the lowest frequency and the one with the highest stress/strain levels.

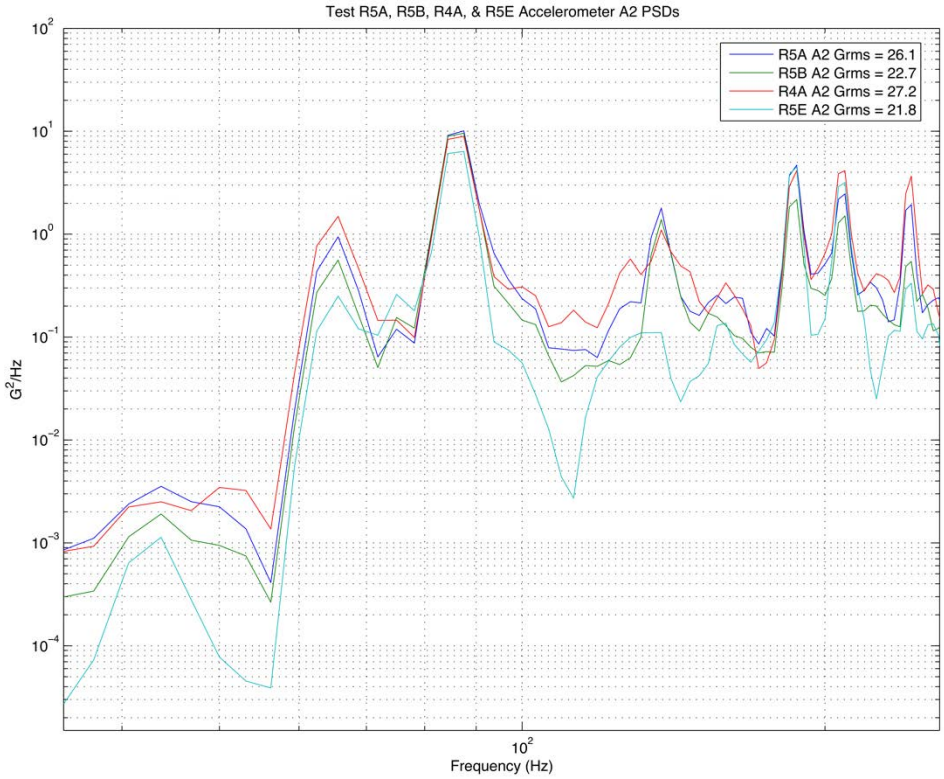

Fig. 27: A2 PSD Comparison for Tests R5A, R5B, R4A, and R5E

The 65.6 Hz resonance in Figs. 26 and 27 shows Test R5B under excites that mode, as compared to what is seen for Tests R5A and R4A. But worse, this behavior is seen throughout the test frequency range for both A1 and A2, which is also seen in the following response discussions. Additionally, Test R5E under excites every mode.

3. Response PSDs for A3 and A4 as a function of Tests R5A, R5B, R4A, and R5E

Again, Test R5A does a better job of exciting the resonances shown by Accelerometers A3 and A4. Test R5A is the only test able to excite and identify the resonance at 203.1 Hz, which is masked by the skirts of the resonance at 209.4 Hz, as shown in Fig. 29.

Figs. 28 and 29 also show that Test R5B again under excites the structural resonances throughout the frequency range for both A3 and A4. This is particularly evident by the responses between 35 Hz and 200 Hz with respect to A4, which is even worse for Test R5E. Test R5B also does not excite the resonance at 137.5 Hz at all, and instead shows a "phantom" resonant peak at 140.6 Hz shown by the tagged cursor at that frequency for the trace that represents the test in Figs. 28 and 29. These result for Test R5B shows that exciting a structure with a non-diffuse field can either reinforce the structural response at a non-resonance frequency, which causes "phantom" resonances, or cancel the response at bona fide resonances (response enhancement and cancellation), which is what causes the notch at 137.5 Hz and the peak at 140.6 Hz that the response of A4 during Test R5B that both Figs. 28 and 29 illustrate.

The first three modes are also better excited by test R5A, as compared to Test R4A, which under excites the lowest resonance at 43.8 Hz, showing a dip instead of a peak (response cancellation) and showing a "phantom" resonance at 53.1 Hz (response enhancement), as shown in Fig. 28. Test R4A also creates an even worse situation for the resonance at 137.5 Hz, where instead it has a dip at 137.5 Hz and instead excites a "phantom" resonance peak at 128.1 Hz (as in Test R5B) appearing, as highlighted by the tagged cursors in Fig. 29, at those two frequencies (response enhancement and cancellation), for the trace corresponding to Test R4A.

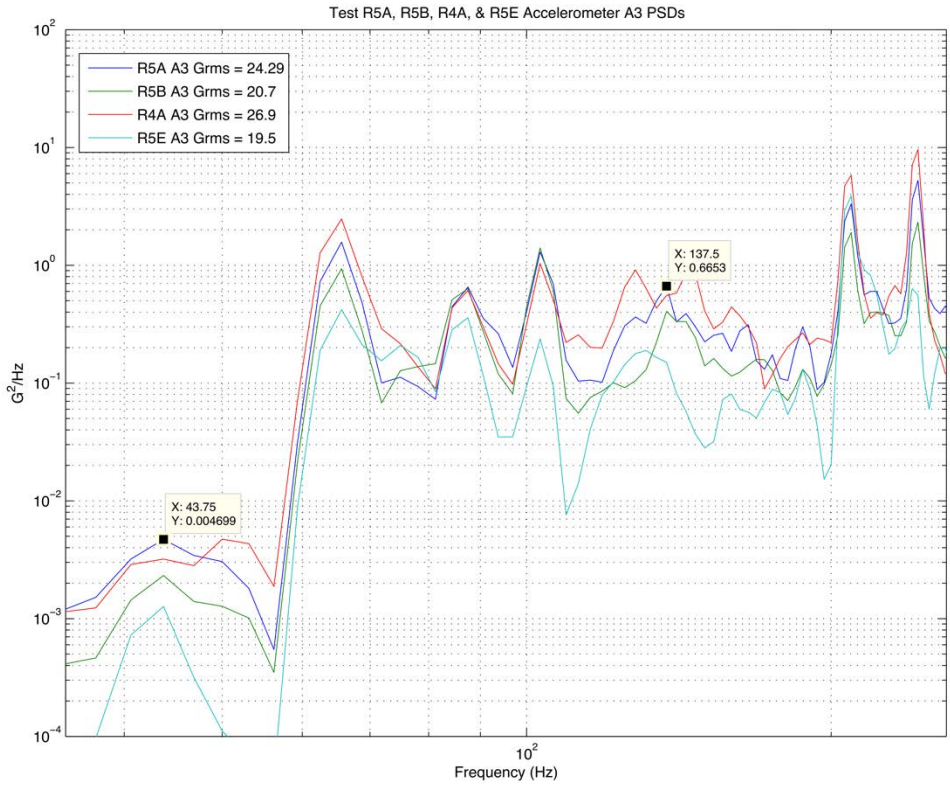

Fig. 28: A3 PSD Comparison for Tests R5A, R5B, R4A, and R5E

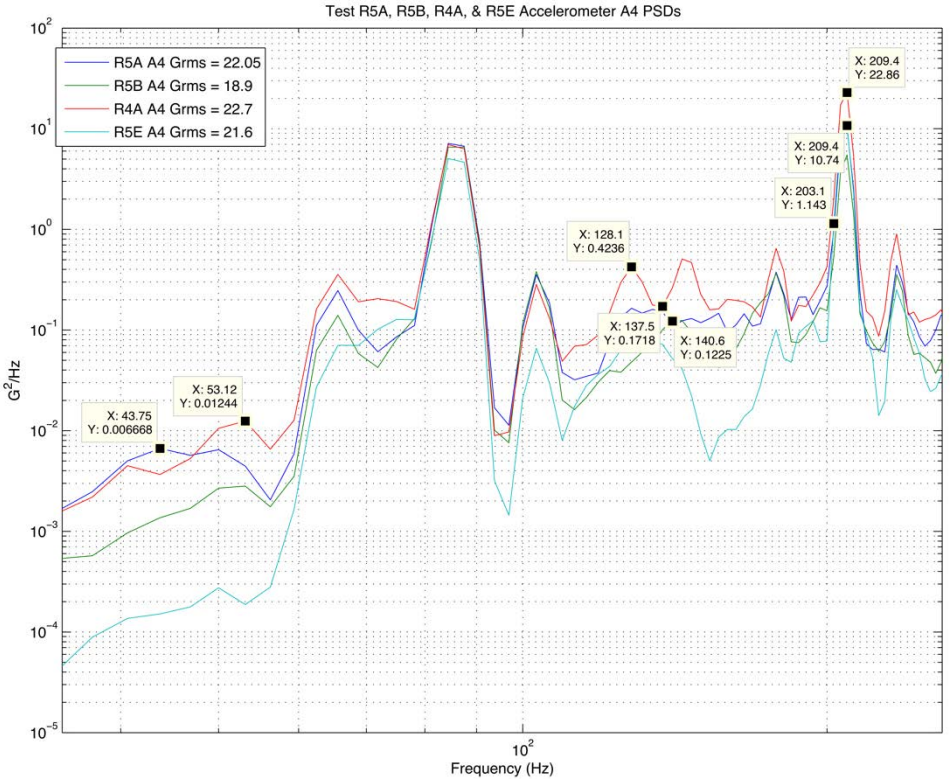

Fig. 29: A4 PSD Comparison for Tests R5A, R5B, R4A, and R5E

Furthermore, on the resonances that Test R4A does excite, many are driven harder (response enhancement) than needed, as the two tagged cursors at 209.4 Hz in Fig. 29 that compare the results from Tests R4A and R5A amply demonstrate. These results for Test R4A clearly show that the results of exciting a structure with a directed coherent field can either reinforce or cancel the response at affected resonances, as was explained previously, which causes the frequency bifurcation displayed for A3 and A4, e.g., at 137.5 Hz. These results also support the existence of a directed coherent field between 50 Hz and 144 Hz with Test R4A, as was previously discussed.

However, this behavior by Tests R5B and R4A notwithstanding, Test R5E is again noticeably the worst performer in general, as compared to the other 3 tests, particularly Test R5A. This is a prime reason why in reference [4], MISO DFAN (DFAT™) testing is not recommended.

4. Response PSDs for A5 and A6 as a function of Tests R5A, R5B, R4A, and R5E

Test R5A is again shown to be better test than R5B, R5E, and R4A in exciting the first three resonances seen by A5 and A6 below 100 Hz and around 137.5 Hz by Figs. 30 and 31, as was discussed in conjunction with the Figs. 28 and 29. Also, higher frequency resonances are more clearly defined by Test R5A than they are for the other 3 tests as seen previously.

Again, the MISO Test R5E is in general the worst performer in these Figures, by under-exciting most of the significant resonances below 300 Hz that are studied by this paper.

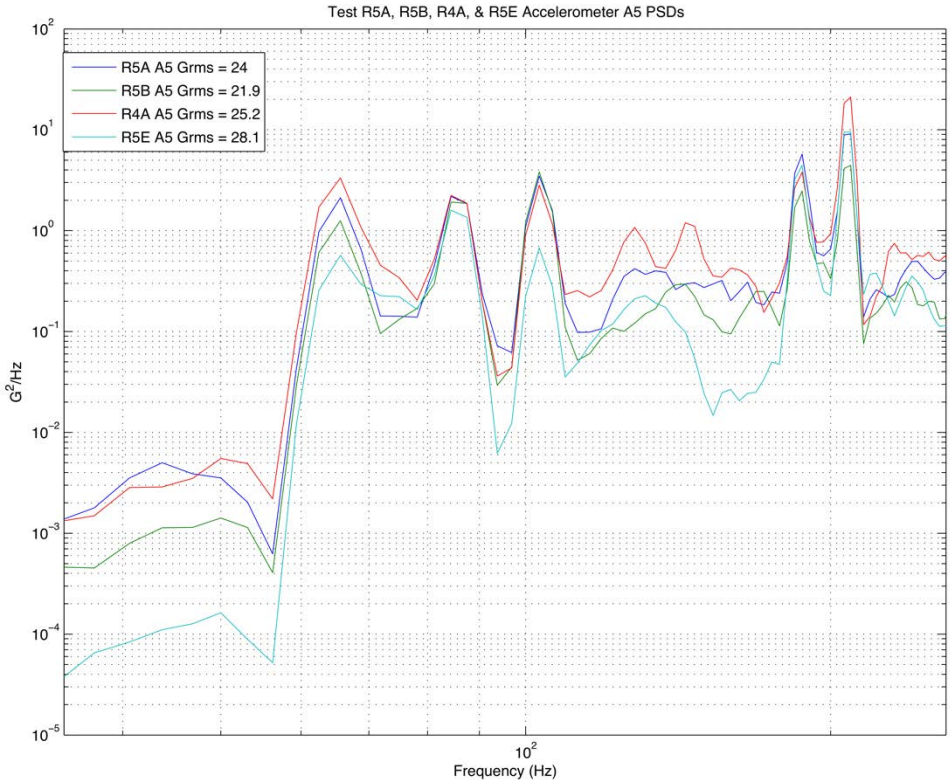

Fig. 30: A5 PSD Comparison for Tests R5A, R5B, R4A, and R5E

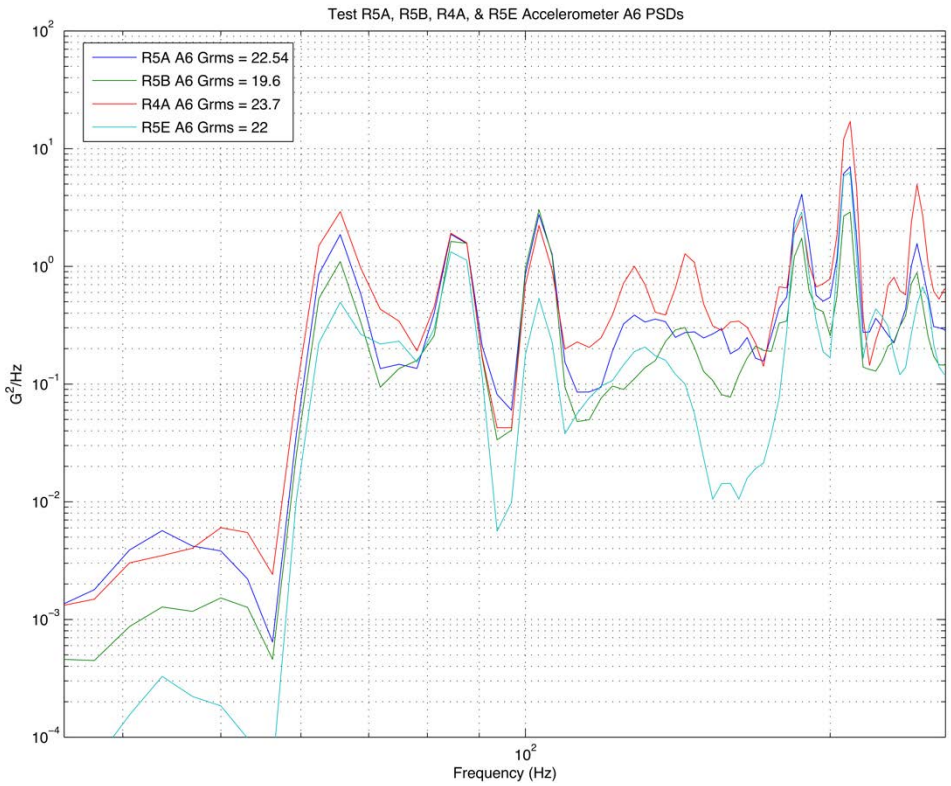

Fig. 31: A6 PSD Comparison for Tests R5A, R5B, R4A, and R5E

5. Response PSDs for A7 and A8 as a function of Tests R5A, R5B, R4A, and R5E

Test R5A clearly identifies the first 4 resonances better than Tests R5B, R4A and R5E, particularly the most important resonance at 43.8 Hz, in the PSDs for A2 through A8. Tests R5B, R4A and R5E miss properly identifying the resonance at 137.5 Hz, with the same problems (response enhancement and cancellation) in Figs. 32 and 33 that were discussed for Figs. 30 and 31, which are again not present for Test R5A. The data shows that Test R5A does a better job than other tests in identifying the 16 resonances.

For example, Test R4A again shows the high sidelobe below the resonance at 137.5 Hz and its cancellation in both Figs. 32 and 33, while showing a "phantom" resonance below it (response enhancement and cancellation). Similar problems occur around 43.8 Hz, 65.6 Hz, and 84.4 Hz with Test R4A. These results are again consistent with directed coherent field excitation to 144 Hz and again validate the earlier conclusions drawn on Test R4A.

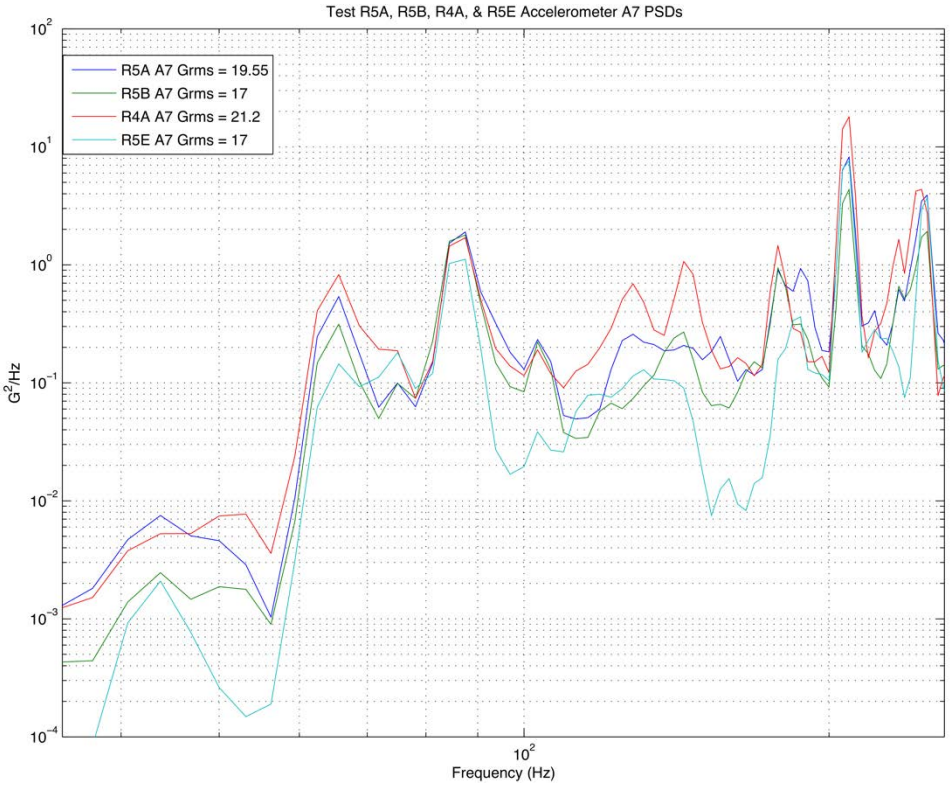

Fig. 32: A7 PSD Comparison for Tests R5A, R5B, R4A, and R5E

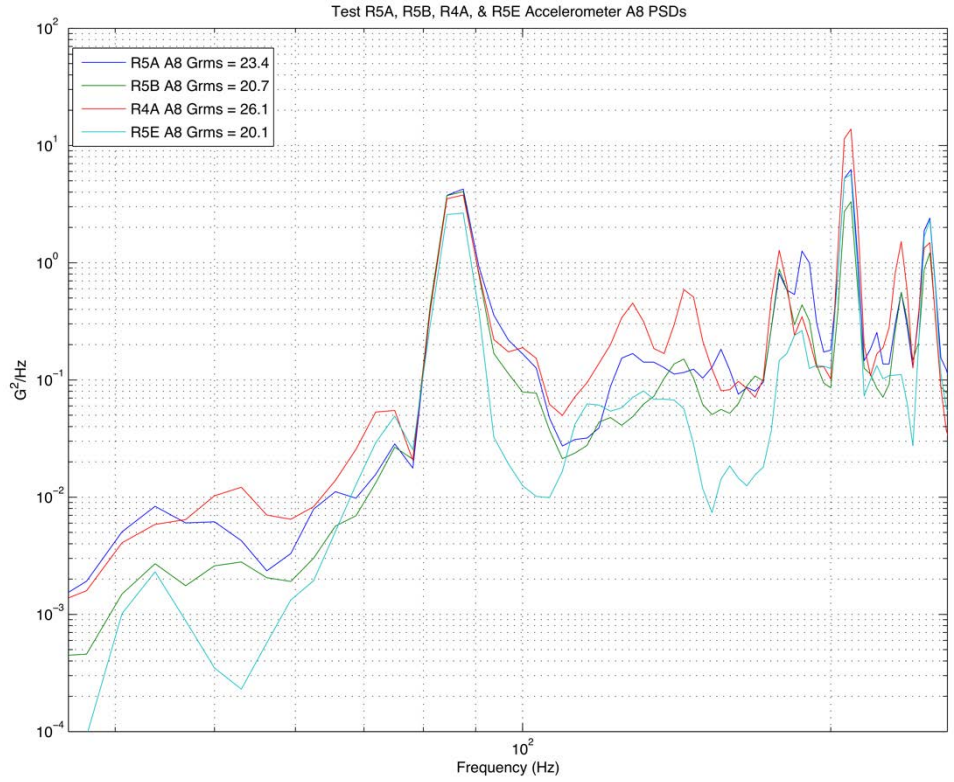

Fig. 33: A8 PSD Comparison for Tests R5A, R5B, R4A, and R5E

Test R5B, on the other hand, misidentifies the 137.5 Hz resonance as being at 140.6 Hz for Accelerometers A3 through A8. It also has similar problems around 43.8 Hz and 84.4 Hz, as was discussed previously for Test R5B.

Again, MISO Test R5E is the worst performing test for identifying the panel's resonances.

6. Response PSDs for A9 and A10 as a function of Tests R5A, R5B, R4A, and R5E

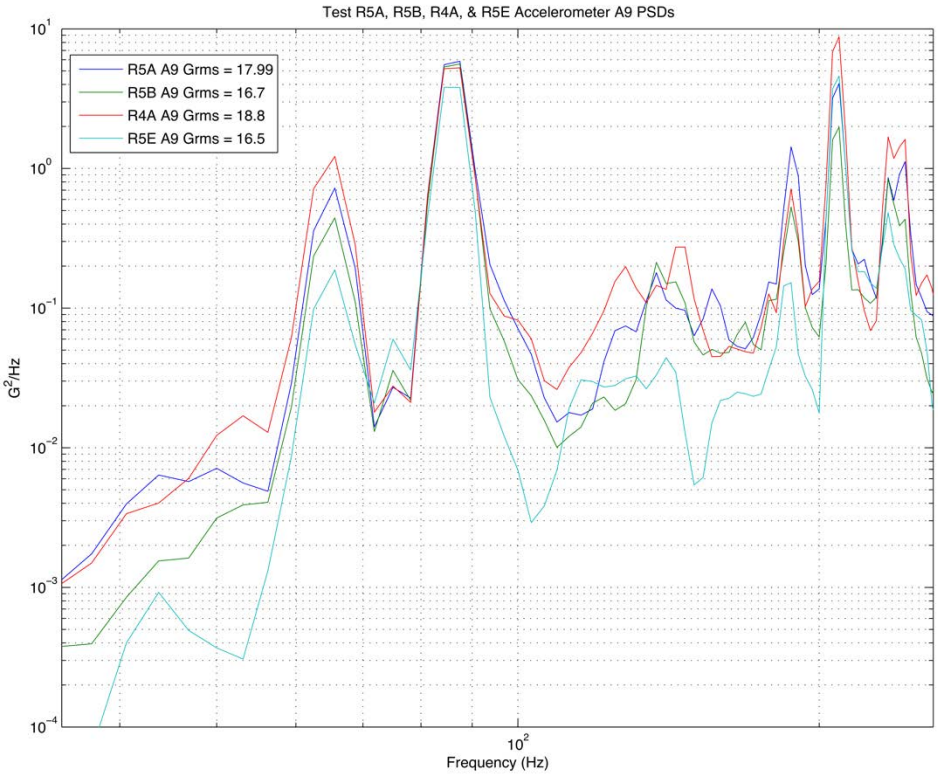

Fig. 34: A9 PSD Comparison for Tests R5A, R5B, R4A, and R5E

Once more, R5A is the top performer in identifying the lowest frequency 43.8 Hz resonances for A9 and A10 as shown for Figs. 34 and 35. The following Fig. 35 shows the cursor on 43.8 Hz, whereas the peak that test R4A shows is at 53.1 Hz, which is a "phantom" resonance. Fig. 34 shows a similar result for the lowest frequency resonance, i.e., a peak at 43.8 Hz for test R5A, but none for Tests R5B and R4A. Test R5E, on the other hand shows a peak at 43.8 Hz, but under-excites it as compared to R5A, as shown by both Figs. 34 and 35.

Tests R5B and Test R4A exhibit the same type of problems with their PSD responses, for A9 that have been discussed previously. However, again for Test 4A as shown by Fig. 35, it shows no peak at 137.5 Hz, which Test R5A does show.

However, A1 and A10 responds better for all Tests R5B and R4A, except at the problem frequencies that have been noted for those Tests. The better response for Tests R5B and R4A for A1 and A10, is probably due to their locations on the edges of the panel. Despite that advantage, Tests R5B and R4A shows many of the same response enhancement/cancellation problems seen previously and MISO Test R5E remains the poorest performing test for this pair of Accelerometers.

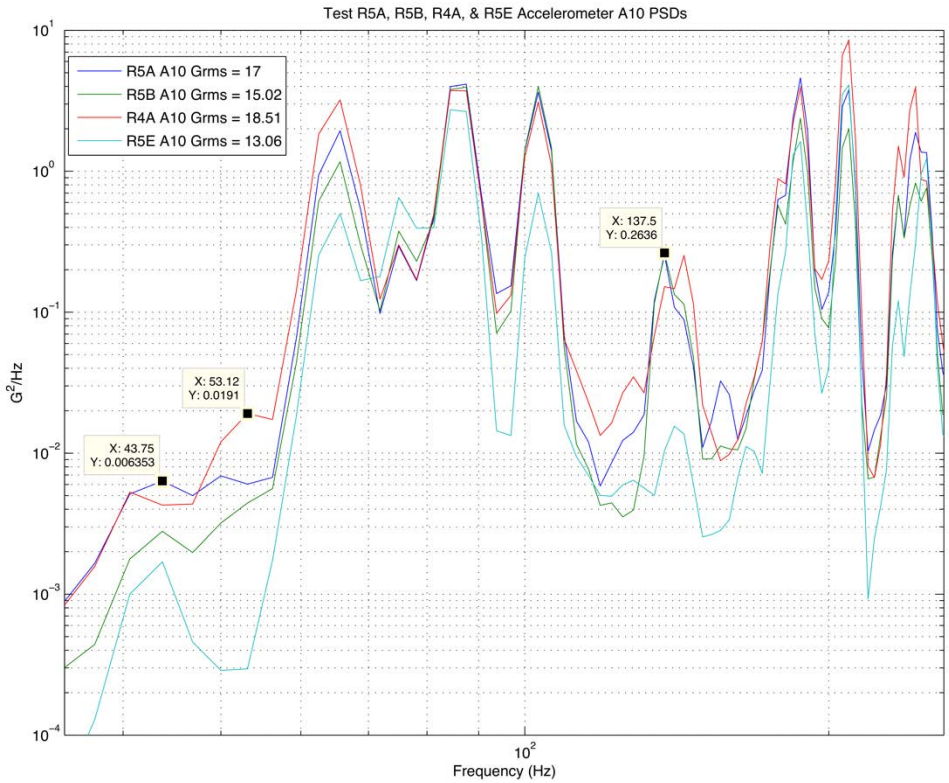

Fig. 35: A10 PSD Comparison for Tests R5A, R5B, R4A, and R5E

VI. Conclusions on Panel Response Comparisons and in General

The previous analysis demonstrates that only test R5A can consistently excite the resonance around 137.5 Hz and as well as the first 6 resonances better than tests R5B, R4A and R5E. It also demonstrates that MISO Test R5E is noticeably the poorest performer as compared to Tests R5A, R5B, and R4A for all 10 accelerometer PSD comparisons that were made.

This result underscores how important the specification of relative coherence and phase between microphones and how well the control system is able to match these specifications used to control the dynamics of an acoustic field are in determining the structural response of a test article during an acoustic test [4,14] and further validate the recommendations of [4] to not use non-diffuse acoustic fields and those created by MISO control for DFAN (DFAT™) testing.

The structural response results for Test R4A support the view that the directed coherent field excitation created by that test was effective to 144 Hz, as was discussed during the analysis of the resulting relative control coherence and phase coherence and phase between control microphones during that test.

The general conclusions from this analysis are that: 1) only the diffuse acoustic field Test R5A properly excites and identifies all the structural resonances; 2) the non-diffuse Tests R5B, R4A, and R5E consistently miss exciting significant resonances properly and many times find “phantom” resonances; and 3) for the resonances that R5A and that one or more of the other tests also excite, diffuse Test R5A excites those resonances more sharply and correctly, and more importantly, shows no “phantom” resonances [4,14].

Consequently, this paper’s major conclusion is that the achieved SDM coherence and phase [9,14] between microphones of an acoustic field used to excite a test article are the most significant factors, in addition to the test’s OA SPL and reference spectrum, that determine its structural response induced by an acoustic test using that field, as has been shown by this response study.

VII. Power Utilization as a Function of Testing Configuration

The following 12 tests listed in Table 2 had their power utilization parameters recorded. These were: Max Drive Vrms Levels and Subwoofer Voltages. There were several variations in the testing configuration that affect these values, such as: the type of MIMO, 8 or 4 drives, whether panel is rotated, coherence specifications, and whether MISO is being used. Table 2 lists the test's power consumption parameters that were obtained for each listed test and its configuration in its various columns.

Table 2: Testing Power Utilization, Test Type, and Power Use Comparison

Test title	Max Drive Vrms	avg. sub Volts	Test Full Level (dB OA)	Test type	coh	Power Ratio (dB)	Power Ratio dB-Reference
R1A	0.27	67.813	138.5	8 Drive MIMO Rotated Panel	0	-0.191	R5A
R1B	0.272	66.063	138.5	8 Drive MIMO Rotated Panel	0.6	-0.127	R5A
R1C	0.243	77.563	138.5	MISO Rotated Panel	N/A	-1.106	R5A
R2A	0.258	76.125	138.5	4 Drive MIMO Rotated Panel	0	-0.586	R5A
R2B	0.277	83.063	138.5	4 Drive MIMO Rotated Panel	0.6	0.031	R5A
R5A	0.276	69.063	138.5	8 Drive MIMO	0	0.000	R5A
R5B	0.282	73.333	138.5	8 Drive MIMO	0.6	0.187	R5A
R5C	0.26	71.25	138.5	4 Drive MIMO	0	-0.519	R5A
R5D	0.278	76.292	138.5	4 Drive MIMO	0.6	0.063	R5A
R5E	0.224	83.958	138.5	MISO	N/A	-1.813	R5A
R4A	0.279	71.75	138.5	8 Drive MIMO	directed coherent field	0.094	R5A
R4B	0.242	66.909	138.5	4 Drive MIMO	directed coherent field	-1.142	R5A

1. The Power utilization and associated configurations of the 12 Tests that were run

Table 2, provides, via its "Power Ratio (dB)" column, values that provide a useful measure of the effect of all of these parameters on the power being utilized for all 12 tests, by using the test's Max Drive Vrms discussed previously referenced to Test R5A, where all of the tests were run using the same reference spectra shown in Fig. 1a. The "avg. sub volts" column provides another useful power utilization parameter to drive the subwoofers in Fig. 1b.

Table 2 lists the maximum drive Vrms and Sub Voltages that were used to run a test, to provide another indication of power utilization as a function of the speaker types used in the 8x8 stacks shown in Fig. 1b for each test. All of these testing results were recorded from the 12 tests that were run.

In what follows we will refer to the values that are shown in the column "Power Ratio (dB)" as "power" and the values in the "avg. sub volts" column as a qualifier of the utilized power for the analysis of each of the 12 tests that are discussed in what follows, since the maximum of most acoustic tests is in the subwoofer frequency range.

The "Power Ratio (dB)" column contains the ratio in dB of two max. drive Vrms ("power") values, the test's max. drive Vrms divided by a chosen test's max. drive Vrms, as a Power Ratio dB reference, for each of the 12 tests that were performed. The "Power Ratio dB Reference" contains the test name used as the test's max. drive Vrms reference, which for this analysis was always the Test R5A, which was the 8-drive incoherent test that was previously discussed.

2. Overall Power Utilization Conclusions from Table 2

    - The "power" saving by going from the incoherent 8-drive MIMO test R5A to the MISO test R5E was about 1.8 dB, which is less the than the 3 dB that others in promotional material have reported previously (not referenced), but which comes with a significant 14.9 V increase in sub Voltage.
    - Going from incoherent MIMO test to highly coherent MIMO test R5B actually costs additional power, although only 0.59 dB, but with 4.3 V increase in the sub Voltage.
    - However, going from an incoherent 8-drive MIMO test R5A to a similar 4-drive MIMO test R5C does save 0.52 dB, which is conventionally run for MSI DFAT customers, but with only a moderate 2.2 V increase in the sub Voltage.
    - It's interesting that that test R5C only has a 1.29 dB "power" penalty over the R5E MISO test, but a significantly smaller sub voltage (12.71 V less).
    - Another interesting fact is that directed coherent acoustic field settings 8-drive MIMO test R4A needs only 0.094 dB more power than the incoherent 8-drive MIMO test R5A and a moderate 2.7 V increase in sub voltage.
    - The overall conclusion is that the incoherent 4-drive MIMO test R5C that is typically run for MSI DFAT space industry customers does not have a significant power penalty (1.3 dB more), as compared to MISO, and that using sub voltage as the metric, uses significantly less power than a MISO test (i.e., 12.7 V less), both of which are substantially less than what others have reported. However, test R5C has the same diffuse field structural resonance excitation advantages over Test R5E that R5A has.

References:

1. *Hannan, E. J., "Multiple Time Series," John Wiley, New York 1970*
2. *Jacobsen, Finn; Roisin, Thibaut, "The coherence of reverberant sound fields," Acoustical Society of America. Journal, March 2000*
3. *Kolaini, Ali, et al., "Acoustically Induced Vibration of Structures: Reverberant Vs. Direct Field Acoustic Testing," 25th Aerospace Testing Seminar, October 2009*
4. *National Aeronautics and Space Administration, "NASA TECHNICAL HANDBOOK: NASA-HDBK-7010—2016-02-01," NASA, February 1, 2016.*
5. *Underwood, Marcos A., "Adaptive Control Method and System for MultiExciter Swept-Sine Testing," U.S. Patent No. 5,299,459, April 5, 1994.*
6. *Underwood, Marcos A., "Adaptive Control Method and System for Transient Waveform Testing," U.S. Patent No. 5,517,426, May 14, 1996.*
7. *Underwood, Marcos A., "Applications of Computers to Shock and Vibration," Shock and Vibration Handbook,*

5th Ed., Chapter 27, Edited by Harris, C. M., and Piersol, A. G., McGraw-Hill, New York, 2001
8. *Underwood, M., and Keller, T., "Rectangular Control of Multi-Shaker Systems; Theory and some practical results," Journal and Proceedings - Institute of Environmental Sciences and Technology, April 2003*
9. *Underwood, M., and Keller, T., "Understanding and using the Spectral Density Matrix," 76th Shock and Vibration Symposium Proceedings, Oct. 2005, Destin, Fl.*
10. *Underwood, M. and Keller, T., "Using the Spectral Density Matrix to Determine Ordinary, Partial, and Multiple Coherence," Proceedings of the 77th Shock and Vibration Symposium, October 2006, Monterrey, CA.*
11. *Underwood, Marcos A., "Digital Control Systems for Vibration Testing Machines," Shock and Vibration Handbook, 6th ed., Chapter 26, Edited by Piersol et al., T. L., McGraw-Hill, New York, 2009*
12. *Underwood, Marcos A., "Applications of Digital Control Techniques to High Level Acoustic Testing," 31st Aerospace Testing Seminar; Oct. 2018; Los Angeles, CA*
13. *Underwood, Marcos A., "Applications of MIMO Digital Adaptive Control to High Level Acoustic Testing," 26th International Congress on Sound & Vibration; July 2019; Montreal, Canada*
14. *Underwood, Marcos A., "New Method Determines Optimized Reference SDM for MIMO Testing," 32nd Aerospace Testing Seminar, October 2021*
15. *Larkin, P., Goldstein, R., and Underwood, M., "Direct Field Acoustic Test System and Method," U.S. Patent No. 9,109,972, filed May 27, 2011*

Biography:

Marcos A. Underwood has a Ph.D. in Electrical Engineering, with specialization in control and communication systems, and a Masters in Mathematics, both from the University of California in Los Angeles. He also has a Masters in Structural Engineering from San Jose State University. His Bachelors, in Mathematics and Physics, is from the California State University in Los Angeles. Dr. Underwood worked with Philco-Ford Aeronutronic, Rockwell International Space Div. on the Space Shuttle project, and Hughes Helicopters on Structural Dynamics and Acoustics, early in his career, developing the use of digital vibration and acoustic control and analysis systems. Later, he also worked with SD, GenRad, STI, and again with SD as their systems architect, designer of their vibration and acoustic control and analysis systems over the years. Afterwards, he held the positions Chief Engineer, V.P of Engineering, and Chief Scientist at STI and SD. During the three phases, he developed some of the fundamental digital technology now used for vibration and acoustic control and analysis. He has been involved in the use, design, and development of digital control and analysis systems for vibration and acoustics for almost 50 years and holds many key patents in the field. He has authored many publications, is a Fellow of the IEST, and the chair of the recommended practices IEST-RP-DTE 022 working group committee on Multi-Shaker Testing and Control. He currently works, from his consulting firm Tu'tuli Enterprises, with MSI DFAT as their Chief Scientist.